FliPASED
WWW.FLIPASED.EU

D5.4 12 month Progress Report

GA number:	815058
Project acronym:	FLIPASED
Project title:	FLIGHT PHASE ADAPTIVE AERO-SERVOELASTIC AIRCRAFT DESIGN METHODS

Funding Scheme: H2020 **ID:** MG-3-1-2018

Latest version of Annex I: 1.1 released on 12/04/2019

Start date of project: 01/09/2019 **Duration:** 40 Months

Lead Beneficiary for this deliverable:	SZTAKI
Author(s): Virag Bodor, Balint Vanek (SZTAKI)	
Last modified: 02/03/2021	**Status: Delivered**
Due date: 30/10/2020	

Project coordinator name and organisation:	Bálint Vanek, SZTAKI
Tel. and email: +36 1 279 6113	vanek@sztaki.hu
Project website:	flipased.eu

Dissemination Level:		
CO	Confidential, only for members of the consortium (including the Commission Services)	
PU	Public	x

"This document is part of a project that has received funding from the European Union's Horizon 2020 research and innovation programme under grant agreement No 815058."

Glossary

ASE	Aeroservoelastic
AFS	Active Flutter Suppression
CAD	Computer-aided Design
CPACS	Common Parametric Aircraft Configuration Schema
DLM	Doublet Lattice Method
FE	Finite Element
GLA	Gust Load Alleviation
LPV	Linear Parameter-varying
LPI	Linear Time-invariant
MDAx	MDAO Workflow Design Accelerator
MDO	Multidisciplinary Design Optimization
MIMO	Multi-Input Multi-Output
MLA	Manoeuvre Load Alleviation
PID	Proportional-Integral-Derivative
RCE	Remote Component Environment
ROM	Reduced Order Model
TCL	Tool Command Language
W3C	Wold Wide Web Consortium
XDSM	Extended Design Structure Matrix
XML	Extensible Markup Language
XSD	XML Schema Definition

Table of Contents

1 Summary for Publication

1.1 Summary of the context and overall objectives of the project

Flight Phase Adaptive Aero-Servo-Elastic Aircraft Design Methods (FliPASED) opens a completely new dimension for the integrated aircraft design. Coupling between aeroelasticity, gust response, flight control methods, instrumentation and certification aspects is not exploited in current aircraft design. A common set of models, coupled with joint requirements enable a multidisciplinary-optimized design for the entire aircraft, leading to more optimized overall performance. The concept of exploiting coupling between disciplines will take advantage of tools developed by the partners in former projects. The main objectives of the proposal aim at tightly coupled multi-objective optimization of advanced, active controlled wing designs through the integration of a collaborative design tool chain. More than 10% fuel efficiency improvement, and 20% reduction in peak amplitude of the gust response, as well as a 50% reduction of number of distinct models used during the development and certification process are set as project goals. Through the integration of all discipline tools from aerodynamics, structural design, aeroelastic simulation and control design in one integrated tool chain an active, condition optimized wing design becomes feasible, enabling enhanced performance at lower weight and cost. The project will raise the efficiency of a currently separately existing development toolchains, by advanced multidisciplinary and collaborative capabilities for whole aircraft along its life cycle. It will develop methods and tools for very accurate flexible-mode modelling and flexible aircraft control synthesis, in the context of reliable implementation of the avionics system, taking into consideration the fault detection and reconfiguration. The accuracy of developed tools and methods will be validated on a safe and affordable experimental platform, and results will be shared along with design requirements and standardized interfaces in an open source approach.

The goal of this project is to develop an advanced design toolchain and novel methods for constructing a demonstrator aircraft that satisfies the key requirements defined for the future aerial vehicles. The simulation based virtual design and assessment of a highly coupled, actively controlled aero-structure will be complemented with extensive test data generated with the flexible wing demonstrator aircraft established in the EU FLEXOP project. Providing extensive ground and flight-testing data will support the tool chain validation as well as providing the international research community real life test cases to check and improve their models and methods.
The following 3 main research objectives are proposed:
1. Raise the efficiency of a currently separately existing wing design, flight controls and avionics development toolchains by advanced multidisciplinary and collaborative capabilities for overall aircraft designs along their life cycle [28]. According to preliminary flight test result by NASA, optimization algorithms and actively shaping the wing found trim configurations that required approximately 3 percent less fuel flow than utilizing baseline trim conditions at the same flight condition (Peak-Seeking Optimization of Trim for Reduced Fuel Consumption: Architecture and Performance Predictions: J. Schaefer and N.A. Brown), if using advanced

flight control augmentation. Key component to this goal is to treat all flight control surfaces uniformly with the consequence of certification aspects still utilizing the multi-functional capabilities to actively control a wide range of conditions of the aircraft.

2. Develop methods and tools for very accurate flexible-mode modelling and flexible aircraft control synthesis, in the context of reliable implementation of the avionics system, taking into consideration the fault detection, isolation and reconfiguration mechanism in failure cases. It is expected that better sensing and advanced control methods can lead to 15% reduction in peak amplitude of the gust response (Introduction to Aircraft Aeroelasticity and Loads: J.R. Wright, J.E. Cooper). Special emphasis will be made on recommending standardized methods and tools across design and certification teams to significantly reduce the number of different mathematical models (50% reduction is sought) leading to more efficient engineering and management effort via better capturing the synergies between multiple disciplines. Through intelligent implementation of reduced order models in the design process also massive reaction time reductions of complex simulations and models are expected.

3. Validate the accuracy of developed tools and methods on a safe and affordable experimental platform, developed in a prior H2020 project (FLEXOP), which will also lead to demonstration of the interdisciplinary development cycle. This will facilitate the interaction of structures, flight controls and avionics disciplines. Gust response prediction and mitigation, active wing morphing for fuel consumption reduction and flight envelope assessment in the event of failures will be tested using the existing ground and flight infrastructure of the partners, with a new set of optimised wings and custom sensor and actuator arrangement. It is foreseen that significant cost can be saved by only manufacturing an advanced set of flexible, aeroelastically tailored wings (supported by shape and loads monitoring) and re-using main components from FLEXOP. In combination with the existing wings sets of the FLEXOP project the overall design space of active flexible wing enabled capabilities will be efficiently expanded, providing a broader and more robust insight into the underlying design and control principles, along the lines of ACARE Action area 2.4 (Secure continued and focused investment). The platform, with its rich sensor and actuator set will also generate vast amount of data, which on the one hand will be handled by Big-Data analytics inside the project and on the other hand will be available through the open data approach for the research and industrial community.

1.2 Work performed from the beginning of the project to the end of the period covered by the report and main results achieved so far

Work has been performed in three technical and one management work packages, while minor preparatory work was also done on the non-active work package (WP4) about scale-up. These work items were the following:

WP1

The wing and demonstrator actuation and sensing concept was reviewed to account for the increased need of sensing and larger amount of actuators coupled with the main objectives of demonstration.

Also the requirements were reviewed to show clear benefits for a/c MDO design, where different advanced functions have to work together in the design phase and their improvement potential has to be quantified.

WP2

Integral part of the MDO toolchain is the flight control system layout, where rigid body, load alleviation, drag reduction and flutter mitigation control laws must work seamlessly. A clear plan and work distribution was established to divide the tasks among partners.

Several already existing tools were adapted for collaborative design, including aircraft overall geometry and structural CAD design, finite element and aeroelastic tools, dynamical modelling and model order reduction, as well as baseline control design. These are all integrated into the RCE execution environment, using the CPACS common description language as a middle layer.

WP3

The demonstrator from FLEXOP had to be revised, including takeoff and landing performance and some of the already existing instrumentation was also revised to provide better handling for pilots and operators. In parallel the flight test program for Flight Test Phase #1 was established with clear goals. Unfortunately, the ground handling of the aircraft and the global pandemic prevented the full execution of the planned tests, but we gained significant confidence and expertise on handling the demonstrator.

WP4

The WP is not active, but due to cross-coupling between demonstrator related MDO and scale-up related design objectives preliminary investigation was done among partners of currently available baseline aircraft configurations and a suitable configuration was chosen, while also fixing the scope of the scale-up MDO task. This will include aero-servo-elastic optimization of the D150 aircraft type (single-aisle, twin engine), but no effort will be devoted to compete with other EU projects where detailed aerodynamic optimization is done using CFD methods.

WP5

Within the management work package the necessary steps to run the project smoothly and in accordance with the EU regulations were established. This includes organizing meetings and providing support for the partners about management related items. The following deliverables have been delivered: Project Handbook, Project webpage and social media, Data management plan.

1.3 Progress beyond the state of the art and expected potential impact (including the socio-economic impact and the wider societal implications of the project so far)

The project achieved significant achievements related to interdisciplinary tool development for MDO processes, especially related to specifying the proper problem setup and the necessary tool adaptation for them. More specifically the consortium developed tools and methods to parametrically define aircraft wing geometry what is also parameterized by the number of flight

control surfaces and integrated this with structural / FEM model development, where aircraft wing parameters are handed over via CPACS common language.

The impact of this twofold: firstly the aircraft design and analysis curriculum at TUM will benefit from these common standard tools and secondly the building blocks and developed tools will be reused in other projects.

The common framework also allows for the inclusion of 3D panel method based aerodynamics, where the same parametric meshing methods (based on CPACS) will be used to provide preliminary induced drag calculation, what is not present with the state-of-art VLM-DLM based tools. This is an essential step in developing aeroservoelastic systems aimed at drag reduction at the early conceptual design stage, where costly CFD calculations are prohibited. The impact of these 3D panel based calculations will be on more refined dynamical model of the aircraft where drag will be also modelled, and the corresponding drag reduction control laws can be incorporated into the dynamical simulation of the aircraft.

Significant effort was also devoted to set-up a generic control design framework with high level of automation, i.e. when the MDO loop generates a new a/c dynamical model the tools should automatically handle the changing dynamics and generate a new control design parameter set, what meets the performance requirements and also feasible from implementation point. This is a new level of model based control synthesis, which is beyond state-of-art, the tools have to be robust for a wide set of input models and have to handle special cases (varying number of unstable poles and zeros).

The demonstrator instrumentation was also significantly revised, which provides more feedback to the operators. The maneuvers for flight test execution are pre-programmed into the flight control computer and the flight test engineer is able to execute these in the order he seems adequate (based on the review of flight test data on the fly). The level of sophistication of the maneuver injection is significantly beyond state-of-art in Academic research projects and would tend to be closer to industry practice. Moreover the secondary flight control computer is also integrated into the onboard avionics, what will have the goal of providing operational modal analysis onboard, what would be a Word's first and a highly relevant achievement for the aerospace community.

The team collaborative effort and common tools are also heavily investigate in the project to catalyze collaboration. A first-generation Hardware-in-the-Loop (HIL) environment is already shared among TUM and SZTAKI with common codebase behind them hosted in Gitlab, and a second generation HIL is under commissioning based on the novel Speedgoat dedicated hardware environment, what will be shared among all partners – providing a truly unique common platform for the entire FLiPASED team, with common code deployment and deep collaboration on code development and testing. This will be a very novel approach to collaborative work within the aerospace domain, helping remote work even during the COVID pandemic.

2 Explanation of the work carried out by the beneficiaries and Overview of the progress (Technical Report 1)

2.1 Explanation of the work carried per WP- Work Package 1

Explain the work carried out in WP1 during the reporting period giving details of the work carried out by each beneficiary involved. As such, WP1 (Recommendations capture and attainment) focuses on derivation of key requirements for the aircraft categories under investigation as well as the interconnection of design tool and the relevant data acquisition and analytics methods and process.

2.1.1 Objectives and activities

The main objective of this work package is to address the complete integrated avionic process including aircraft shape, sensors and actuator locations and detailed control design. The purpose is to set up an integrated collaborative framework and tool-chain for the design of a new passively and actively controlled flexible wing-based aircraft, in a safer and more reliable context. The purpose of the activity is to end-up with an enhanced and fastened maturation process tool to quickly reach high maturity levels through digital-based methods and tools.

- Detailed design of control functions
- Enhancement and maturation of (single discipline) tools
- Setup of integrated tool framework
- Establish integrated, collaborative design tool chain
- Re-Design of FLEXOP -1 Wing established (Validation)
- Design of new advanced active controlled wing
- Establish redundancy based methods for enhanced safety and reliability

2.1.2 Starting point and approach

The two main starting points for this WP are the existing demonstrator design (inherited from FLEXOP), what has to be accommodated into the improved design toolchain, and the existing tools, standards and available scale-up aircraft models of the partners.

The approach consists of assembling the main specifications and criteria what must be demonstrated during the flight tests of the demonstrator and from these specifications the required hardware and software modifications and improved data processing workflow have to be developed in an incremental fashion.

On the other side, the limitations of the current demonstrator has to be established (like low Mach number, lack of wind tunnel and complex CFD testing). Based on these limitations the scale-up study also has to limit its scope, to be aligned with the tools and methods developed by partners.

Besides the existing tools the partners have to agree also on the common standards and workflow, what is highly facilitated by DLR's experience with MDO tools and the related CPACS data interchange language.

2.1.3 Efforts and achieved results, name involved contractors

Within the reporting period a number of changes have been proposed to improve the conceptual design of sensor layout and actuation system of the wing (3), and the improvements made and proposed on the fuselage based on operational experience.

During integration and operation of the aircraft the operation team found a couple of design related problems which either made the operation unsafe like the landing gear, or give too harsh boundary for critical function implementation like the lack of digital remote control interface on the RX-MUX units. Along with that, some additional changes were already made to improve the existing functionality like secondary on board computer, and further changes are proposed to have even increased functionality like electrical power measurement or High bandwidth telemetry system. The deliverable D1.1 introduce these changes in more depth.

The wing (3) sensor layout and actuation system has been also revides and a number of improvments have been proposed and implemented. Along with the inertial measurement units used on previous wings other sensor layout concepts are proposed. On flight control and actuator system side, a CAN bus based actuator system is proposed. Along with that a detailed comparison is given between the proposed design and the system used on previous wings during the legacy FLEXOP project.

The experiences and detailed study on the servo health monitoring system currently used in the -0, -1 and -2 wings have been also revised and improvements have been proposed to increase servo deflection measurements for better system identification.

The main contributions of the team are:

- Collecting the main changes proposed in the fusealge, compared to original design documents

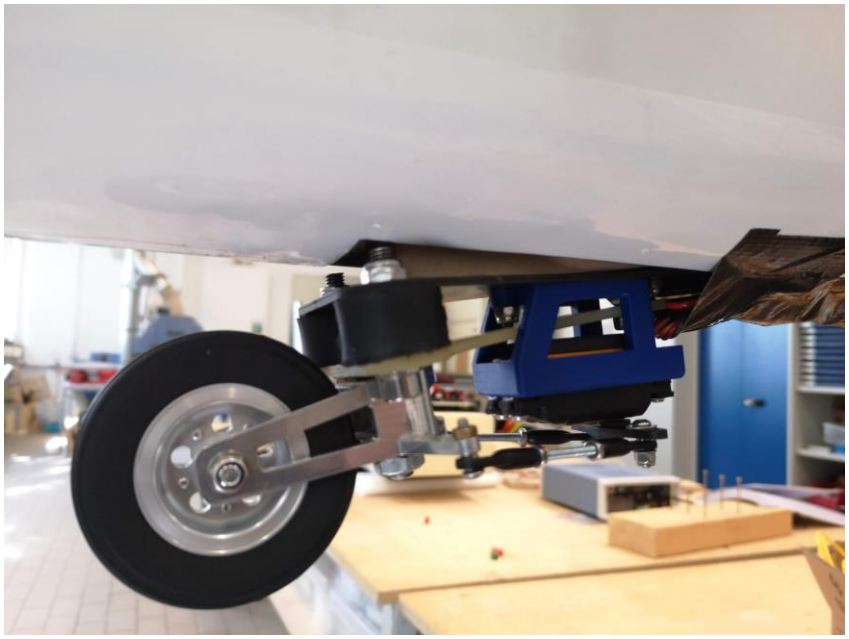

Figure 2.1 modified steerable landing gear

- Providing an updated sensor layout concepts for wing (3).

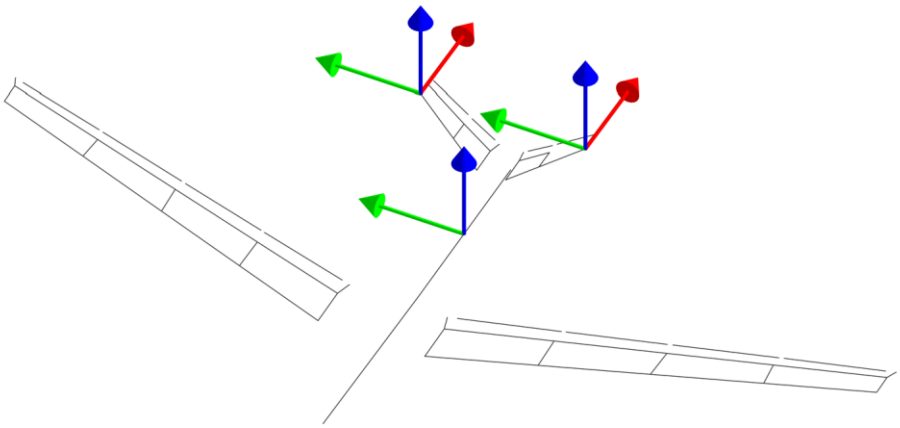

Figure 2.2 Improved onboard IMU locations for tail flexible motion detection

- Providing an actuator system concept for wing (3).
- Showing a detailed analysis of the previously used servo health monitoring tools system.

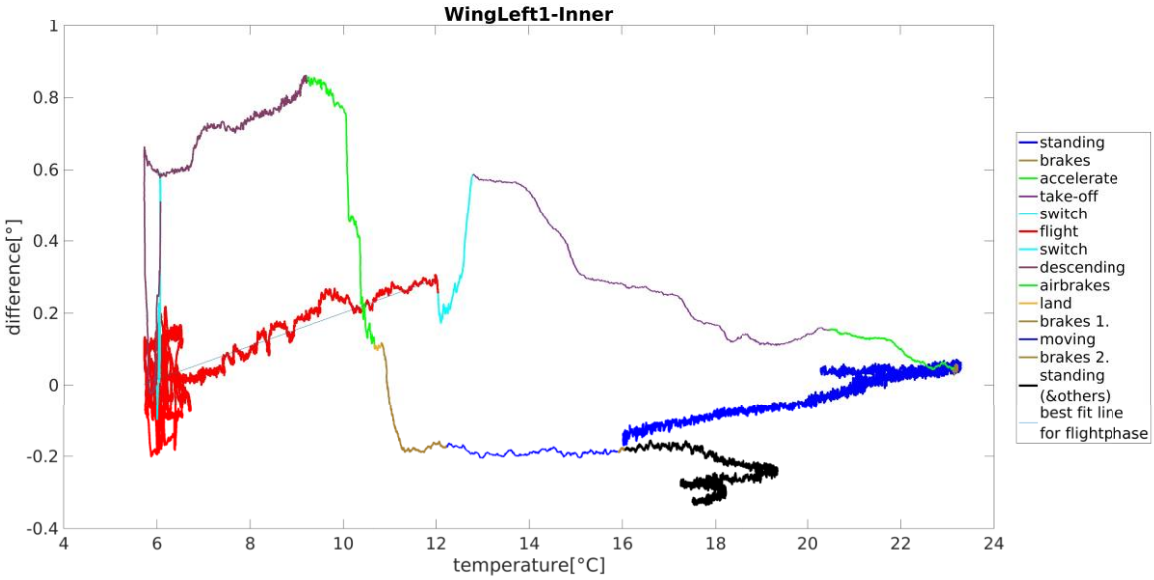

Figure 2.3 Temperature and flight state related calibration of servo deflection feedback

On the overall MDO design loop front in order to set up a collaborative design toolchain for an advanced, actively flight condition optimized wing design, requirements for the MDO toolchain need to be captured first. Deliverable D1.2 captured the outcomes of activities conducted for the requirement capture and serves as the top-level guideline for the subsequent MDO implementation.

The tasks conducted within the period related to setting up the overall collaborative MDO toolchain have been the following:

The objectives of the MDO toolchain and derived requirements were discussed and agreed among the partners. Two sorts of requirements are specified because of the different objectives for demonstrator wing design and commercial transport aircraft wing design.

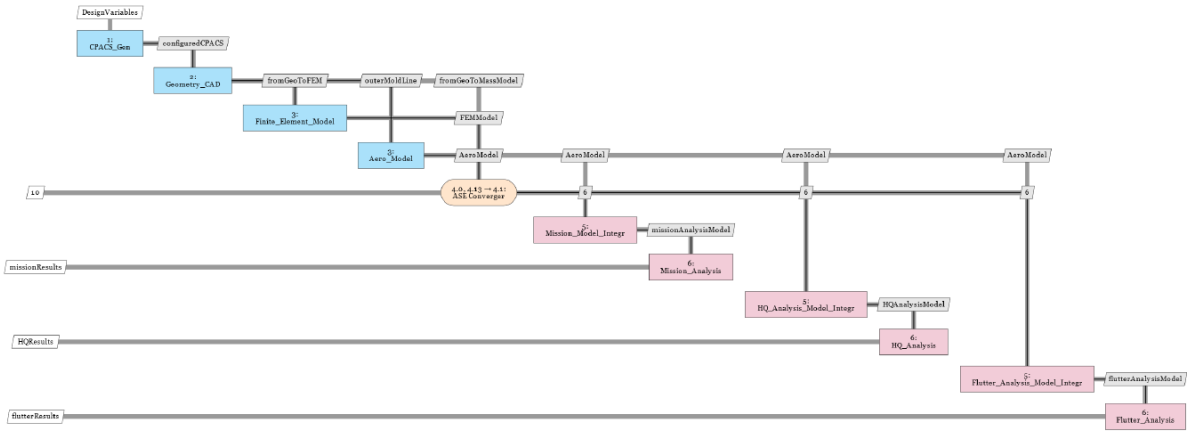

Figure 2.4 MDO worklflow in XDSM format with collapsed 'ASE converger'

The context of the consortium's activities related to the industry standard MDO toolchains were studied. Based on prior project results and experience the MDO toolchain structure is captured by MDAx, which is developed by DLR to support the ideation phase of MDO. The functions of individual blocks are specified and their interconnection has been iterated among the partners. An introduction of the integration framework RCE is given here.

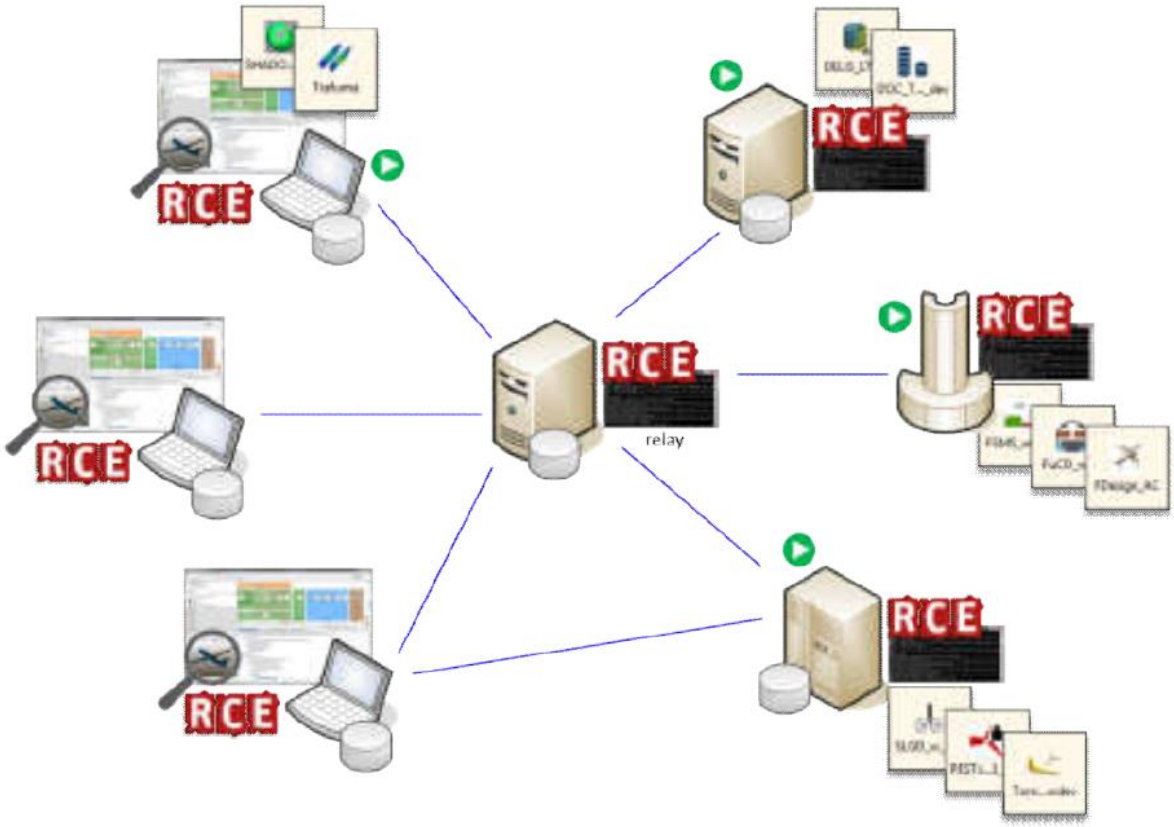

Figure 2.5 Distributed RCE workflow

The definition of interfaces of connected blocks in MDO toolchain required significant effort, due to the multidisciplinary nature of the project and due to the need that each block has to be 'human intervention free', to avoid lengthy hand tuning of parameters by experts within the MDO iteration loops. An introduction to CPACS, which is agreed by the consortium to serve as the standard interface medium, is also given here.

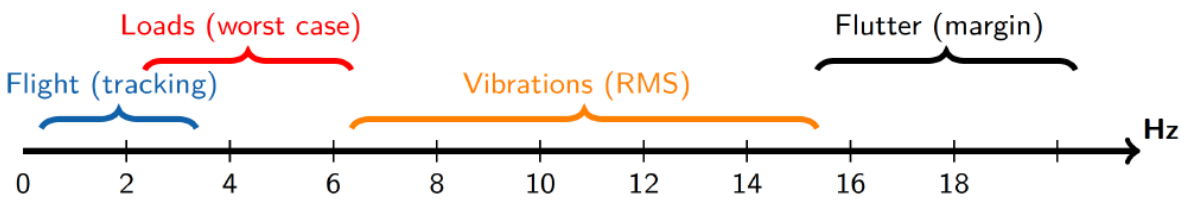

Figure 2.6 Frequency grid of the physical phenomena occurring over an aircraft. Ranges and values are

different from an aircraft to an other.

2.1.4 Deviations, their reason, impact on the project and corrective actions

The project is heavily impacted by the COVID related restrictions, what are even more striking in WP1, since both the hands-on work on the demonstrator has to be postponed several times and the supporting teams of DLR and SZTAKI were only able to be on site at TUM for a very limited time.

On the other hand this facilitated the need of online collaborative tools and methods. What has been established on several fronts: the teams are using common software development repositories using the SZTAKI hosted Gitlab site. The teams also collaborated more closely on developing tools compatible with the CPACS/RCE framework, what can be integrated into the workflow remotely.

Task 1.1: Requirements Capture is mostly done, but on-site brainstorming sessions would highly facilitate the discussions. The team adopted a weekly webex session where dedicated sessions are devoted to requirement capture.

Task 1.2 A/C Reference Model Definition – the team selected a suitable aircraft benchmark, the D150, which is well known and understood by DLR and its limitations are set, to limit the scope of the consortium.

Task 1.3 Collaborative Work Process Definition – based on the CPACS and RCE standards the work process is defined but there is significant delay in the integration of these blocks, since many partners are permanently at home office, where they cannot access the company's main computer infrastructure.

2.2 Explanation of the work carried per WP- Work Package 2

2.2.1 Objectives and activities

Within the FLiPASED project, the Work Package 2 (WP2) is dedicated to the feedback control functions construction. The main objective of the WP is to develop a bundle of functions allowing designing the control functions in an automated manner, in order to be included in the global Multi Disciplinary Optimisation (MDO) process. This MDO being the central objective of FLiPASED.

2.2.2 Starting point and approach

Generally, aircraft manufacturer control design workflow follows what we can call a frequency grid approach. This approach consists in designing different controllers, through a frequency guideline. Each of them address a phenomenon the aircraft is faced during its operation. Within the overall MDO process philosophy, and in this WP, we aim at following this approach also. With reference to figure below, one may notice that different phenomena (flight, loads...) usually occurs around different frequencies.

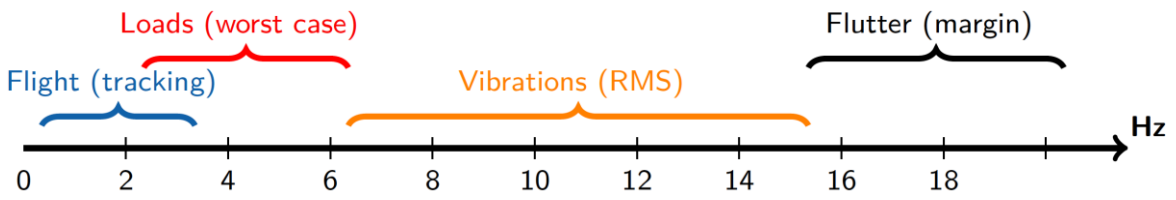

The values of these frequencies are dependent on the geometry and structure of the aircraft, and in the considered case, one may expect even more blending. Still, the big picture remains. This sequential control structure will be kept in mind in the WP2 flow to stick to industrial and practical expectations. The starting point of the project in then this gri line and the know-how of each parteners.

2.2.3 Efforts and achieved results, name involved contractors

During this first year, most of the time and efforts have been dedicated to the expression of the architecture of the flight control system an layout and the way to attack such complete control objective in cascaded manner.

Efforts have been oriented to the definition of the sub functionalities at a granularity level very low and very precise. This description is given in the Flight Control System Layout report (D2.1).

2.2.4 Deviations, their reason, impact on the project and corrective actions

This year, due to pandemic issues and distancing, few functions have been developed in practice. The overall layout seems in a good way, but now, a strong focus on the functions development should be done. This won't have a slowing impact on the project, but (scientific) activities are now on the road.

2.3 Explanation of the work carried per WP- Work Package 3

2.3.1 Objectives and activities

The Work Package 3, Demonstration and Testing, has the following objectives:

- Model refinement using GVT data
- Model refinement using flight tests
- Performance verification of active control methods

In addition, the activities, related to all mechanical work such as manufacturing and integration are also covered by the work package.

Most of the tasks, as defined in the project proposal, are already active. Task 3.1, dealing with preparation of the demonstrator, has seen much activity starting in December, 2019, with planning of the needed upgrades for safe operation of the demonstrator. For the Task 3.2, Demonstrator Wing Design, sensor conpect has been discussed for the new wing design. Task 3.3, Manufacturing and Integration, had activities related to design and manufacturing of a new control module of the Flight Control Computer, the RXMUX. Most of the work has been performed under Task 3.4, Ground Testing of the Demonstrator. This included software updates and integration, multiple taxi tests of the upgraded landing gear and simulator training in preparation for the flight tests. During Task 3.5, Flight Test Specification and System Identification, plans for 1st Phase Flight Test Campaign have been made. Sadly, no actual test flight took place up to now. Therefore, Task 3.6, Flight Test Campaigns, is not yet active.

2.3.2 Starting point and approach

Initial state of the demonstrator (TUM)

The project for TUM has started with a demonstrator, which has already been used in the previous project, FLEXOP. The demonstrator has performed six flight test up to then. However, building on previous experience, landing gear proved to be one of the biggest challenges during the operation of the demonstrator. The aircraft was very difficult to control while on the ground, leading to a few very dangerous situations and one accident, where the aircraft skidded of the runway and hit a runway light. Therefore, upgrades were necesary to ensure sustainable operation of the aircraft.

Figure 2.7. FLEXOP Demonstrator during the last flight previous year.

As a starting point, the following design flaws have been identified:

1. The maximum angle of attack, achieved on the ground, is limited by very low main landing gear and a high tail wheel. This design solution limits the maximum angle of attack that could be achieved for takeoff to 3.3deg. This is very small for a taildragger aircraft and usually would be around 10deg. In addition, fixing such a design on an already manufactured aircraft is not easy.
2. Very narrow main landing gear makes it easy for the aircraft to bank from wingtip to wingtip. If this happens during takeoff or landing, the wingtip touches the ground and instantly creates a destabilizing moment.
3. Main landing gear is longitudinally far from the center of gravity. This means that the disturbing bank angle, required to tip the aircraft, is further decreased.
4. The tires of the main landing gear are too soft for the airplane. This makes it possible to deform the tires very easily and also significantly increases the rolling resistance during take-off run.
5. Unsteerable tail wheel makes the aircraft very hard to control while on the ground. The tail has to be lifted up first and aircraft is then steered with the rudder.
6. Retractable main landing gear proved to be an unnecessary design add-on to the aircraft which adds complexity, but not value to the demonstrator overall.

These problems were hard to identify during the conceptual or preliminary design phase of the FLEXOP project and were only realized during operations. Therefore further discussion was held how to make the controlability of the aircraft better.

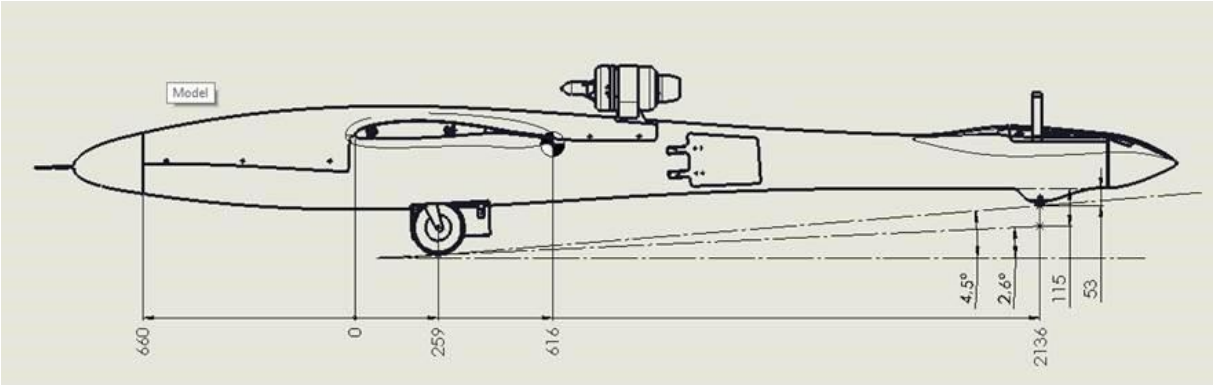

Figure 2.8. Comparison of the maximum angle of attack during take-off. 4.5 degrees is the initial tailstrike angle, 2.6 degrees is the tailstrike angle with steerable tailwheel assembly (wing incidence angle is -1.2 degrees).

Another objective during the first year of the project was to improve the operations of the demonstrator. This was done in three areas: streamline the operational procedures at the airport, change the electronic wiring to decrease number of actions required to set the aircraft up and improve role redundancy within the team. Therefore, further meetings were setup within the flight test team to discuss and streamline the preparation guidelines as well as think about how to make the crew planning easier. In addition, issues were identified in the electrical system of the aircraft that made the complexity of operations higher than it could be.

Since the data, gathered from flight test, had to be processed, some processing toolchains have already been implemented from before. Sensor errors were already being dealt with, as well as logging errors. The end product would be a single file with clear data structure inside that could be used with MATLAB for further analysis. However, the ultimate goal is to streamline the processing of the data as much as possible. This would include a completely automated data processing, where very minimal operator action is needed. In addition, the automated processing would compile a preliminary test report, allowing to analyse the outcome of the test on the fly.

2.3.3 Efforts and achieved results, name involved contractors

Improving the landing gear (TUM)

Two different concepts for fixing the landing gear were discussed:

1. Fundamentally changing the landing gear layout.
2. Adjusting the current landing gear to make it acceptably safe for operation.

Because of the fact that the first option would require major fuselage changes and would take at least a few months, it was decided to start with the second option first. Ways to improve handling were discussed during the winter before the first flight test campaign. Due to the complex nature of the problem the solutions that were initially agreed upon did not completely

resolve the issue. This resulted in an iterative process with different concepts being implemented as add-ons to the initial design along the way. The chronology of the process was:

1. Implement the steerable tailwheel with damping
    a. The initial solution to steering was to install an off-the-shelf tailwheel assembly. Unfortunately, the solution did not work because the load on the tailwheel appeared to be too big for the part. Therefore another, completely custom iteration was done. This included a custom milled aluminum fork for steering and a damping assembly. The damping assembly was composed of glass-fiber-reinforced plastic plate acting as a leaf spring for longitudinal damping and two rubber dampers for lateral stiffness. The structure held well, but the steering made the aircraft hard to control and very sensitive to any pilot inputs.
2. Change the brakes of the main landing gear to more effective ones
    a. Tire brakes were changed to drum brakes. From previous testing it was noted that the tires wear out very quickly due to the brakes. Also, the braking power of the old system proved to be too little. Therefore, new type of brakes was implemented that would both conserve the tires and increase the braking force on the wheel hub.
3. Add a gyro to the tailwheel
    a. Introducing the steerable tailwheel did not solve the controlability problem as the team has hopped. The aircraft became very sensitive, especially at higher speeds. The solution was to introduce a gyroscope-based compensation for the gain on the steering. This proved to improve the steering somewhat.
4. Reverse the main landing gear frame to shift the ground contact point back
    a. One of the main findings, mentioned in the early research on taildragger aircraft is that the tendency to veer of the runway is decreased if the centre of gravity is kept as close as possible to the main landing gear. This was recorded in all the reports on the topic. Therefore, changing the location of the landing gear was considered. Luckily, the landing gear frame was easy to flip, moving the main landing gear backwards by 75mm. The outcome was lesser tendency to veer off the runway, an increase to the critical bank angle to tip on one wing, but also higher load on the main tires. Even though the weight increase was only 2.5% per wheel, the main tires were already overloaded before. The further steps would include looking for stiffer main tires, if possible.
5. Laterally stiffen the main landing gear assembly
    a. During the taxi tests cameras were mounted facing both the gears. This helped to observe the behavior of the landing gear and make further conclusions. One of them was that the main landing gear is too flexible laterally, which makes it easier to tip onto one wing and harder to get out of the tipped position. Therefore, further parts were introduced to stiffen the landing gear laterally.

At the time of writing, the landing gear is still being tested and further improved.

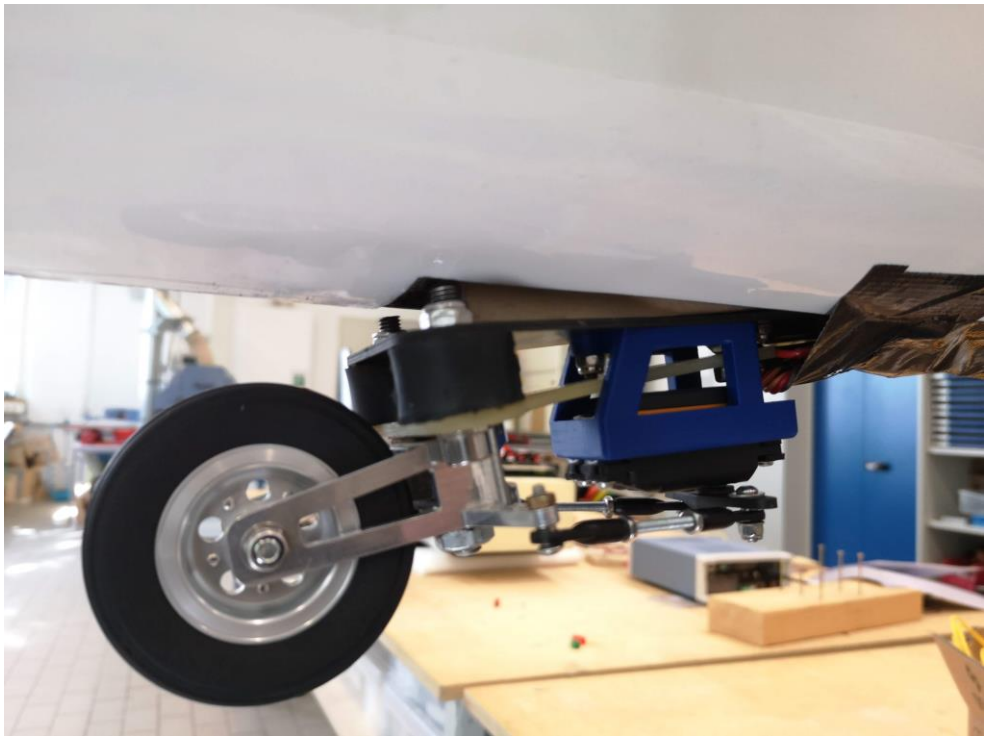

Figure 2.9. Steerable tailwheel assembly.

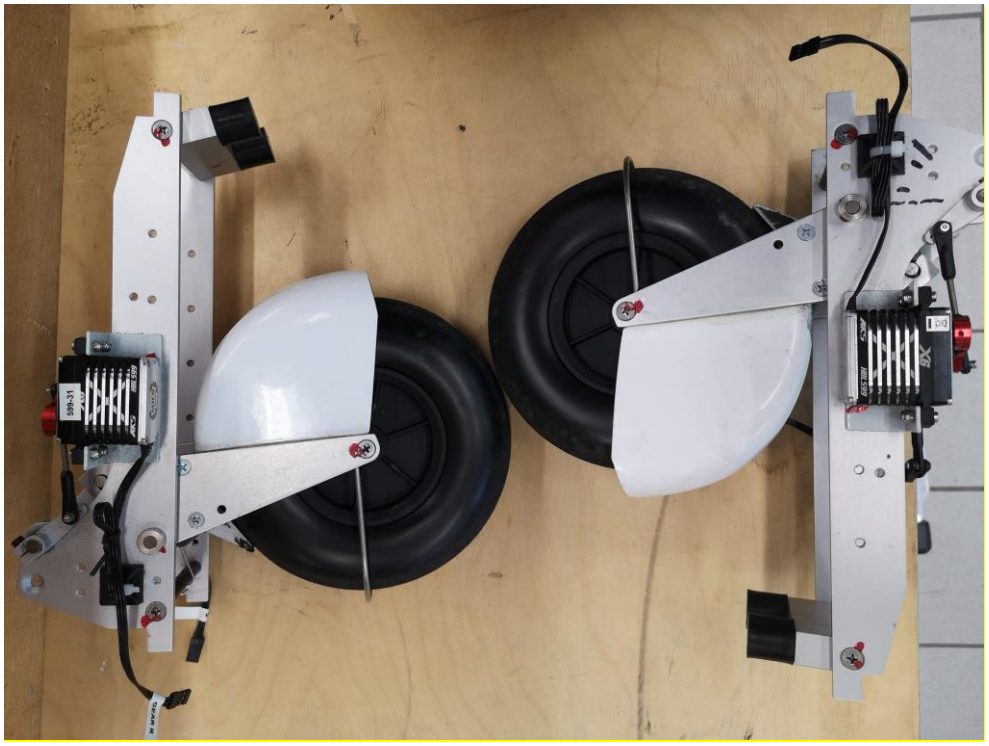

Figure 2.10. Comparison of two possible position for the main landing gear. The difference is around 75mm.

Figure 2.11. Too soft tires deforming under normal load.

Flutter damper mechanism (TUM)

Another activity that relates to preparing the demonstrator for flight test campaign is the development of an emergency solution for the upcoming flutter tests. The idea was to be able to reduce risk of losing the demonstrator by creating a device that would completely change the resonant frequency of the flutter wing (-1), stopping it for flutter. The pilot would trigger this device in case of extreme wing flutter. Currently, the device is being designed and tests are being planned for the upcoming winter.

Improvements in electrical system (TUM)

Past flight tests showed the need for the ability to put the FLEXOP demonstrator into a power-saving stand-by mode that allows extended waiting times with quick reaction times to use unexpectedly opening flight windows. The past efforts addressed these two issues.

In order to implement a stand-by mode for the aircraft, the power consumption of the demonstrator needed to be reduced to a practical amount by selectively shutting down components that feature a high power consumption, should not be operated idle for extended times and/or have a quick und uncomplicated boot-up process. The power supply system has to be capable to either run the remaining components over an extended period of time or capable of keeping the components running while batteries are being swapped. After an analysis of the existing system and iterative review of different possibilities the following measures were decided upon:

1. Adding a circuit breaker in the power line between one 2S-batterie and the power-distribution board.
2. Rerouting the cable supplying the RX-MUX-boards to the splitting point before the circuit breaker.

Thus, in order to put the demonstrator into a power-saving stand-by mode, the following main steps need to be performed:

1. Moving the power switches of the FBG-interrogators to “ÖFF”-position.
2. Disconnecting the 3S battery.
3. Removing the circuit-breaker of the first 2S-battery.
4. Disconnecting the second 2S-battery.

In this state, the 6S-battery is only powering the Raspberry Pie of the FCC flight stack, which can be supplied for several hours. In order to start up the demonstrator for flight tests, the above steps are undone in reverse order.

After the implementation of the changes to the power system, a new landing gear was rigged in. The new landing gear setup features linear actuators for retractiion and deployment, as well as drum brakes that were expected to have a higher holding force and less wear on the tyres than the stamp brakes used before. The b reakes work with three different voltage levels, i.e. 12 V, 7.2 V as well as 6 V. The different voltage levels are supplied by the 3S-battery and the 2S-batteries respectively. In order to provide a supply voltage of 6 V, a DC/DC-converter was introduced that supplied both gear system. During testing the brake servos did not operate reliably. Investigastions on the system yielded a signal-cross-talk from one servo signal line to another. The problem was solved by introduction of another DC/DC-converter.

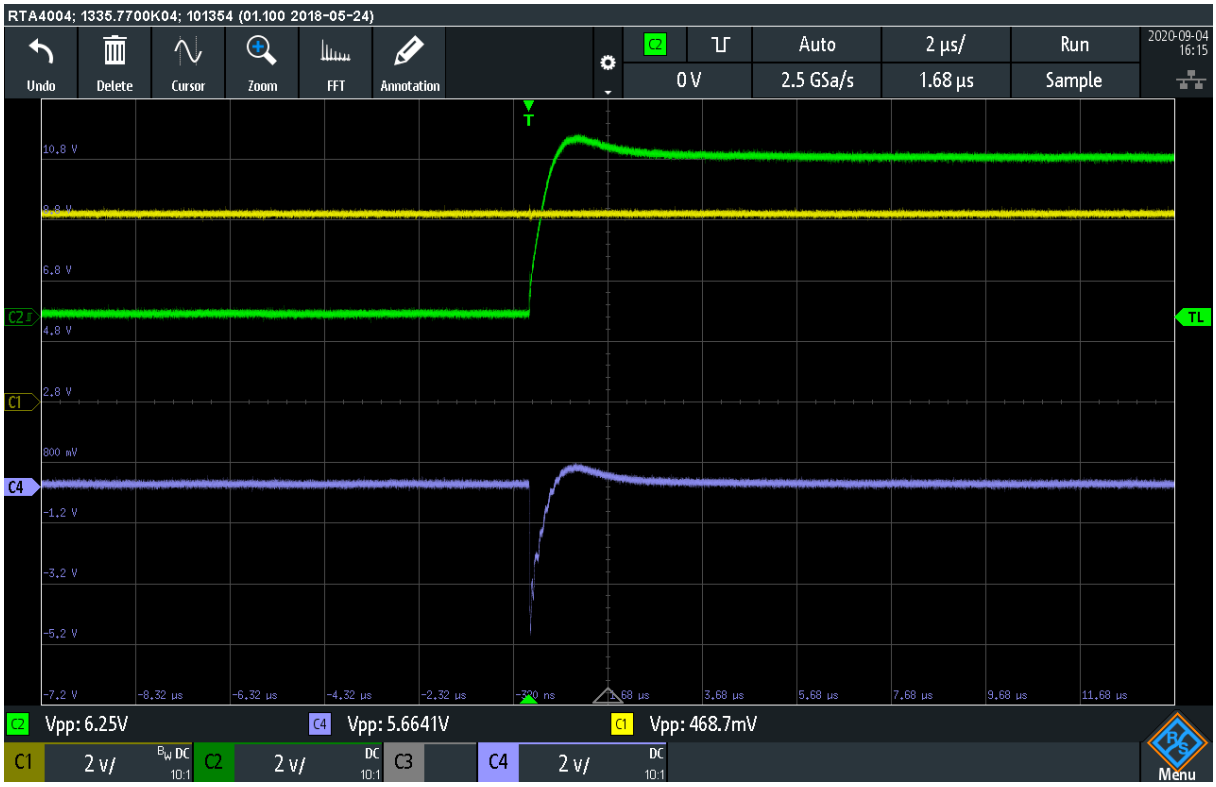

Figure 2.12 - Close look on the cross-talk, when only one step-down converter was used for both actuator. The peak value of the noise overshoots the standard TTL logical threasholds.

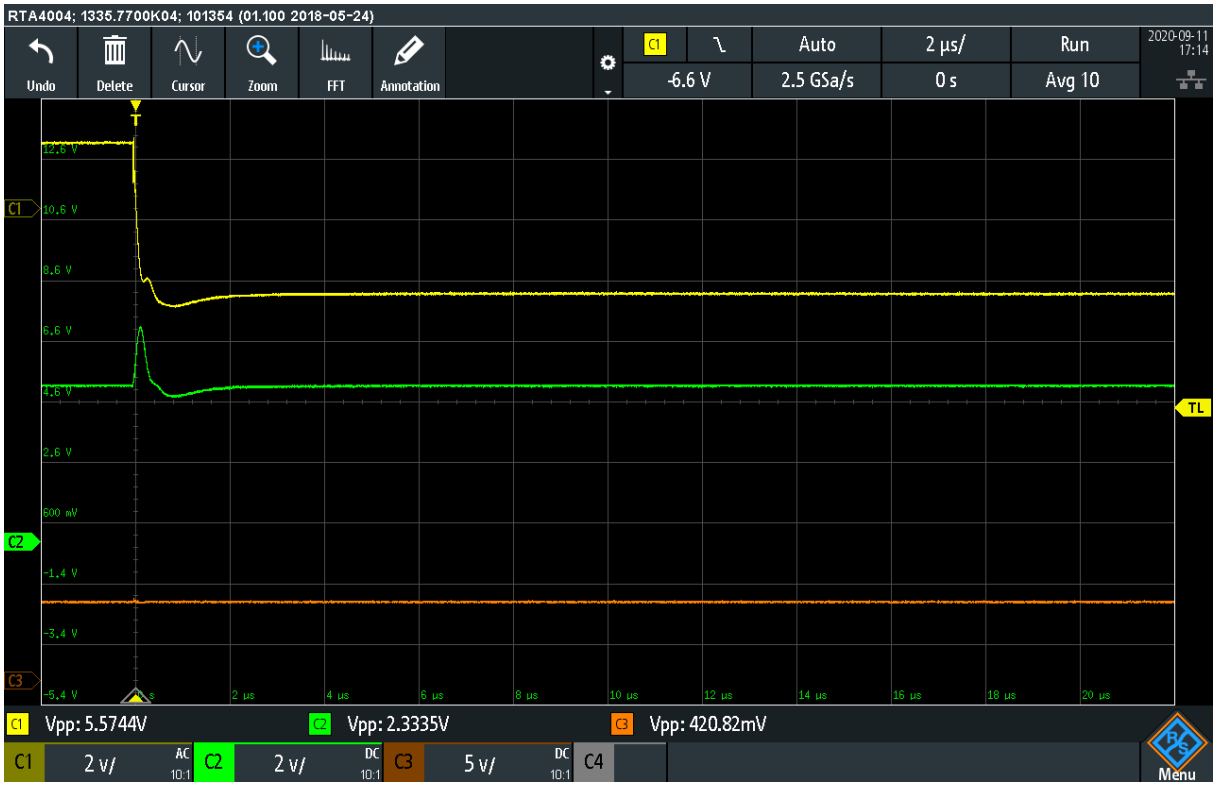

Figure 2.13 - Crosstalk still visible with dedicated step-down converters. The noise peak is still high, but it does not show visible error on the system itself.

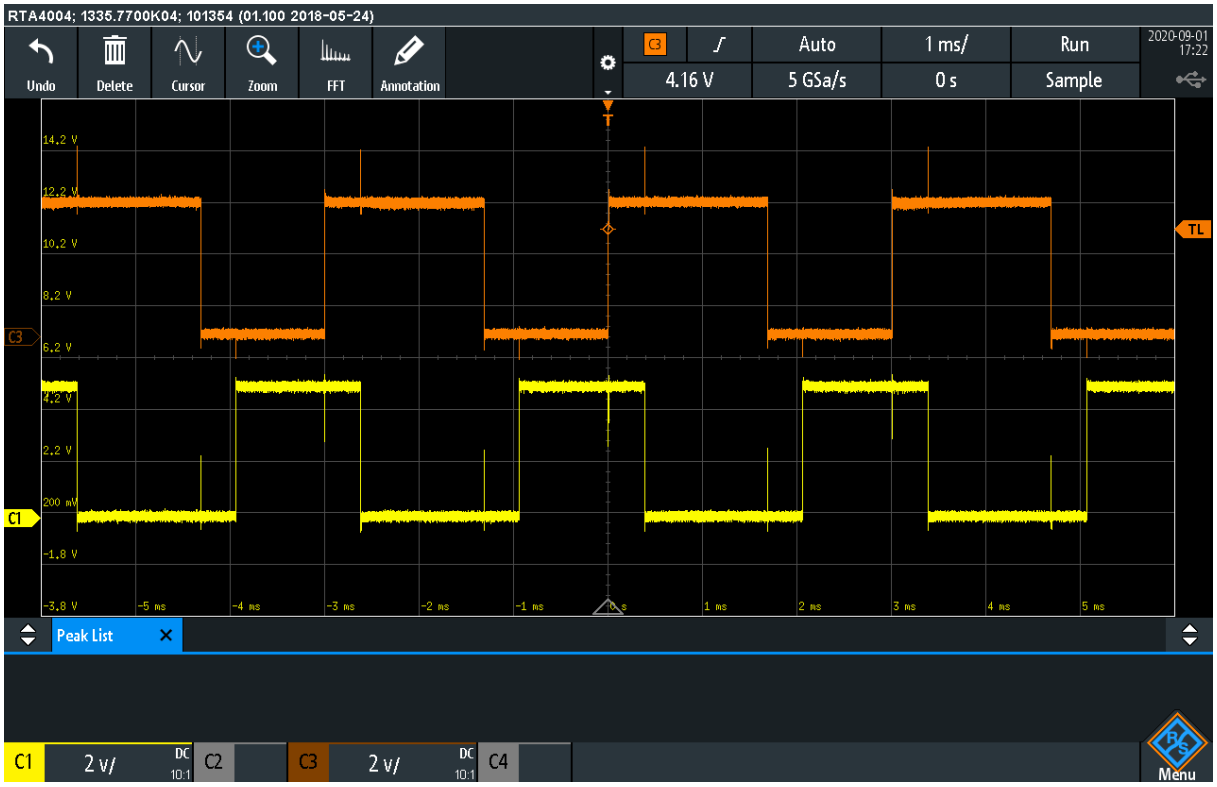

Figure 2.14 - Visible cross talk on the independently generated PWM lines, when actuators are attached.

A seconday on-bard computer was added as well to the FCC stack. That system now runs a program developed by DLR. The secondary on-bard computer is a raspberry pi 4, and it has a direct telemetry connection to the GCS. Currently it run dummy simulation, and provides live telemetry feed to the GCS for testing.

Later, this device will collect all additional measurements provided by newly introduced systems.

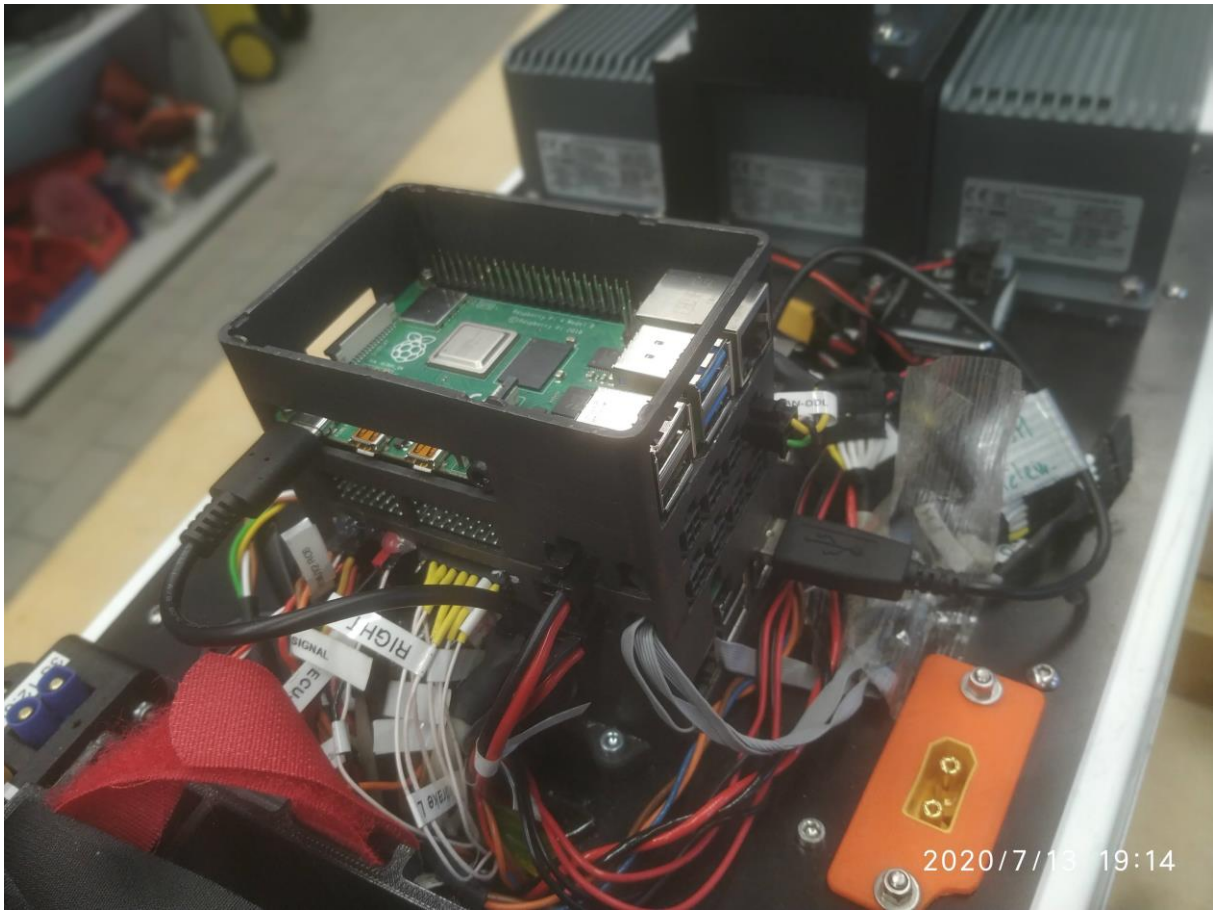

Figure 2.15 - Secondary on-board computer on top of the existing flight-stack.

Improvements in telemetry system (TUM)

Former experience has shown, that the focus of interest in different data sources shifts between flight tests. While initial flight tests focus on system checks, data yielding information about the system performance such as temperatures, currents, voltages and fuel flows are of greatest interest to assure safe flying. With increasing routine and experience with the demonstrator, focus gradually shifts to different data such as airspeed or altitude to attain and keep the planned test conditions or the identification of different mo1des. This shift in focus also manifests itself by the adaption of the data displays and mode of visualization. The current display of the Engineering Data Link developed in Mathworks Matlab does neither offer the necessary flexibility to change display layouts fast nor does it offer a great variety of different modes of display. In order to improve the flight test efficiency by usage of more flexible displays, NASA's OpenMCT framework was implemented and adapted for flight testing of the FLEXOP flight demonstrator. Expected advantages of the new visualization framework are flexible adjustment of data displays, saving of different views that can be switched easily, a wide variety of widgets already available, data "playback" functionality that greatly improves and facilitates flight test debriefings as well as the increase of flight test participants by providing flight data live to remote participants, that can provide additional expertise.

Figure 2.16: Display of NASA's OpenMCT visualization framework during flight tests using the DG-800 S flying testbed.

A working state of August 20 is displayed in the Figure. The moving graphs are widgets that can be adjusted in size and colour as well as types of data displayed.

To date the functionality that has been tested with the FLEXOP flight demonstrator is the display of different modes and normalized eigenfrequencies identified by the secondary Raspberry Pi developed by DLR Göttingen using OpenMCT. Flight monitoring functionality – including safety critical - and flight test adjustment ability has been field-tested and validated using the DG-800 S flying testbed of LLS. This type has great resemblance with the FLEXOP configuration (sailplane with dorsal turbine) and has already been employed for pilot training. Combined with an antenna-tracker, which provides a high-bandwidth connection to the testbed using 5GHz-Wifi, data collected for sytem identification of rigid modes has been streamed down and displayed live in OpenMCT. During flight tests conducted, the reliability and flexibility of the framework was proven: E.g. the data visualization enabled the identification of a sensor failure, which allowed the adjustment of the fight test routine including a change of data displayed. Furthermore, the display proved to be so realiable, that a reduction of safety margins concerning fuel available was possible, which resulted in a near-optimal use of flight time. Initial tests showed the possibility to increase the number of flight test participants by streaming available data to a server, from which it is accessible remotely.

Upcoming efforts will target the implementation of a 5GHz Wifi, high-bandwidth downlink from the FLEXOP flight demonstrator and development of display templates required for future flight tests. Therefore, a Wifi-connection will be established to the secondary RaspberryPie, which will send down data necessary to duplicate the Engineering Data Link. The amount of data will gradually be increased in order to provide flight test relevant data to the operators. On the

hardware-side, integration of servers and an LTE-router are ongoing and will enter consolidation and commissioning phase next.

In order to make full use of the capabilities of OpenMCT, an antenna-tracker was field-tested and commissioned for flight tests using the same DG-800 S flying testbed as employed for testing OpenMCT. The antenna tracker depicted in the figure below.

Figure 2.17: The antenna tracker being prepared for DG-800 S flight tests.

The tracker uses its own as well as the UAV's position to align the antenna to a position facing the UAV in air. During flight tests, 400 values per second were received and processed without experiencing drop-outs. The testcases included distances of 700 m and more, as well as close inverted flybys to test the systems robustness in case a bad GPS-reception. Given the experience of related projects, it can be assumed that the system's capabilities are not maxed out yet.

Therefore, next efforts will focus on further testing of the system as well as increasing the traffic on the data link to use the antenna tracker to its full potential.

Testing the Flight Control Computer (SZTAKI)

To test the functionalities of the Flight Control Computer and its software with the autopilot before flight tests, we performed tests in Hardware-in-the-Loop test environment and on the real aircraft as well. To select the required autopilot functionality, we created a graphical interface which managed by the test engineer in the groun control station.

The main autopilot functionalities we tested:

- Baseline functions
    - Autothrottle
    - Altitude holding

    - Course angle
    - Waypoint tracking
- Identification functions
    - Signal injection to the engine and control surfaces

Hardware-in-the-Loop tests (SZTAKI)

Baseline tests

For example, you can see how autothrottle test was performed in HIL. Figure 2.18 shows how throttle signal and airspeed changes if we give the following commands:

1. Use RC AP2 (augmented mode + autothrottle, nominal speed 38 m/s)
2. Reference velocity change from 38 m/s to 42 m/s
3. Reference velocity change from 42 m/s to 34 m/s
4. Reference velocity change from 34 m/s to 38 m/s

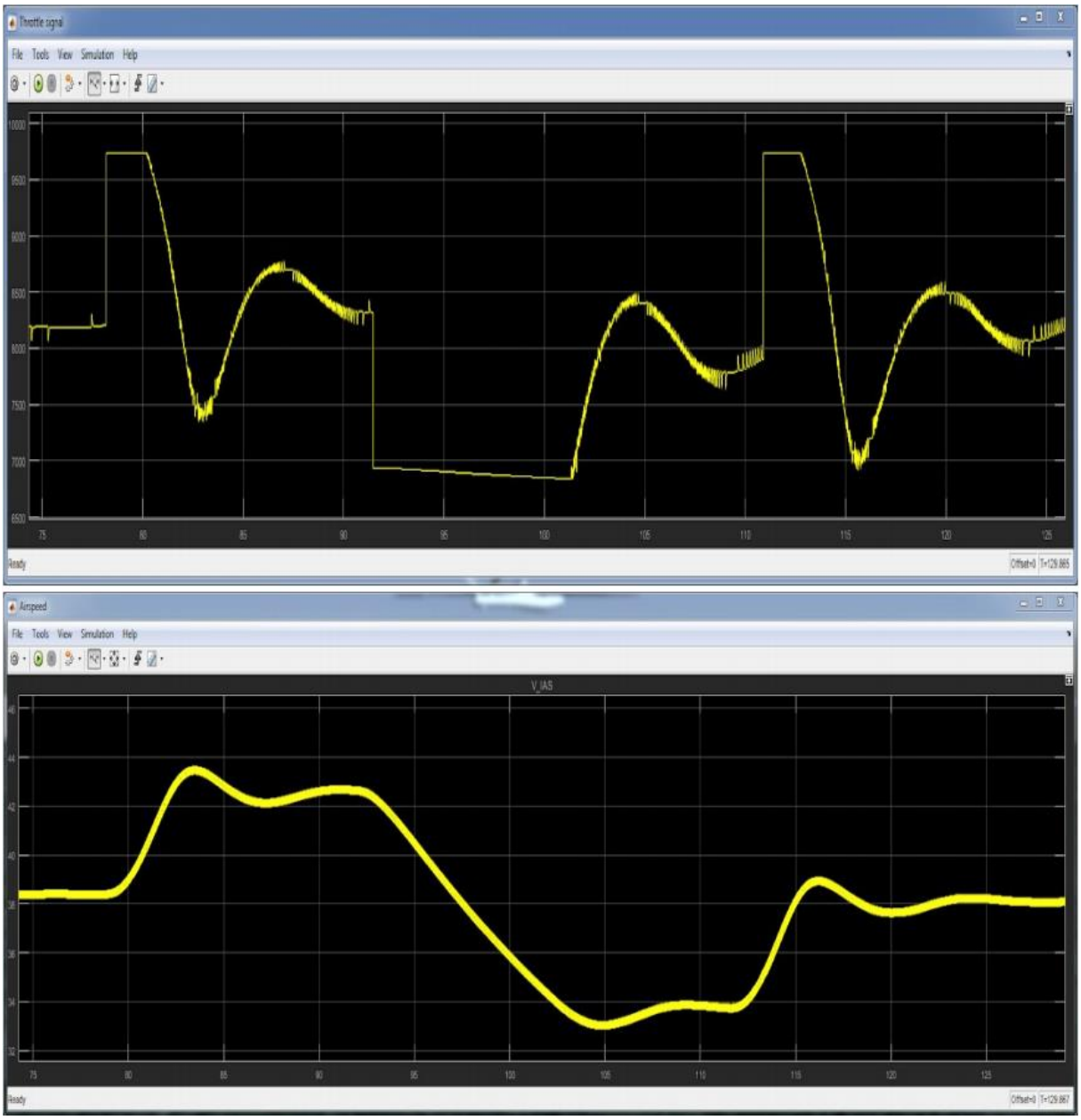

Figure 2.18 – Autothrottle HIL test

Identification tests

In engine identification mode, we inject step signals to the engine. Figure 2.19 shows how airspeed changes with an injected signal.

Throttle injection mode HIL test:

1. Mavlink in Baseline mode, augmented + throttle inject (open loop throttle in this SW_PI version) (velocity panel active)

2. 1st leg: start from RC AP1 trimmed 34 m/s straight and level (inner loop engaged), push 38 m/s button in Mavlink, switch to RC AP2, observe velocity increase with minimum pilot interference (RC throttle stick inactive) then switch back to RC AP1
3. 3rd leg: start from RC AP1 trimmed 34 m/s straight and level (inner loop engaged), push 42 m/s button in Mavlink, switch to RC AP2, observe velocity increase with minimum pilot interference (RC throttle stick inactive) then switch back to RC AP1

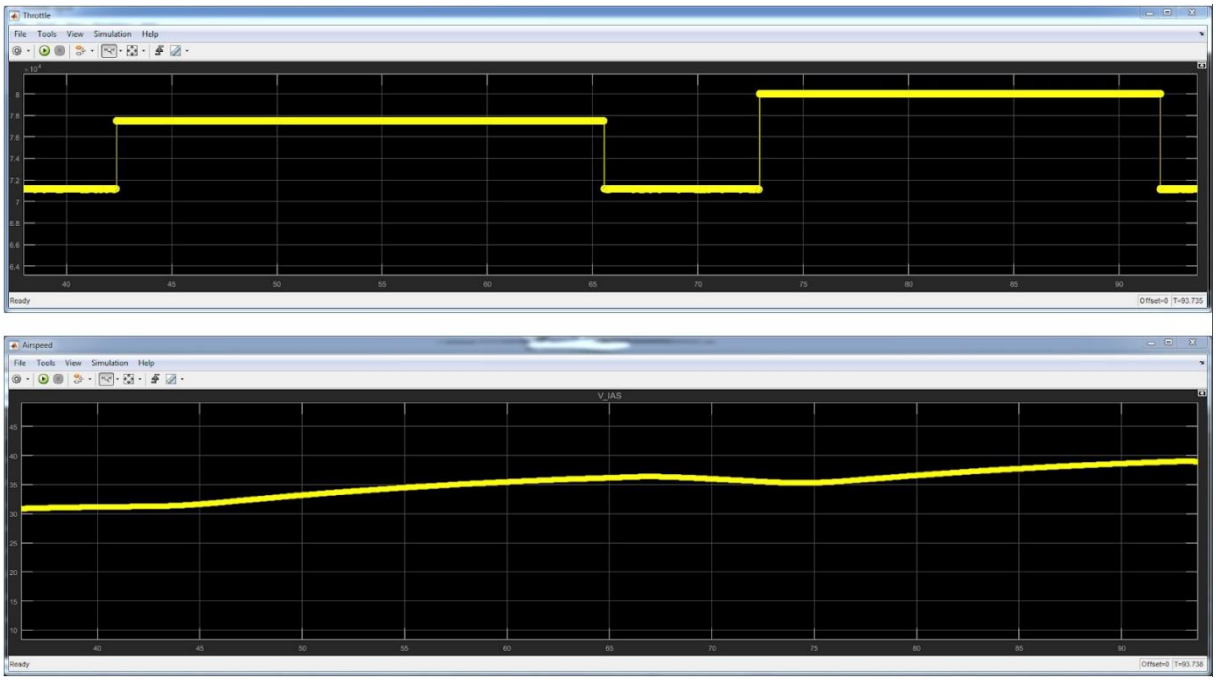

Figure 2.19 - Throttle signal injection HIL test

Signal injection mode HIL test:

1. Select Signal injection mode in Mavlink before flight and select between Flexible and Flight Mechanics tabs
2. Set initial velocity, amplitude multiplier and signal in RC AP1 during flight
3. Switch to RC AP2 to inject the selected signal

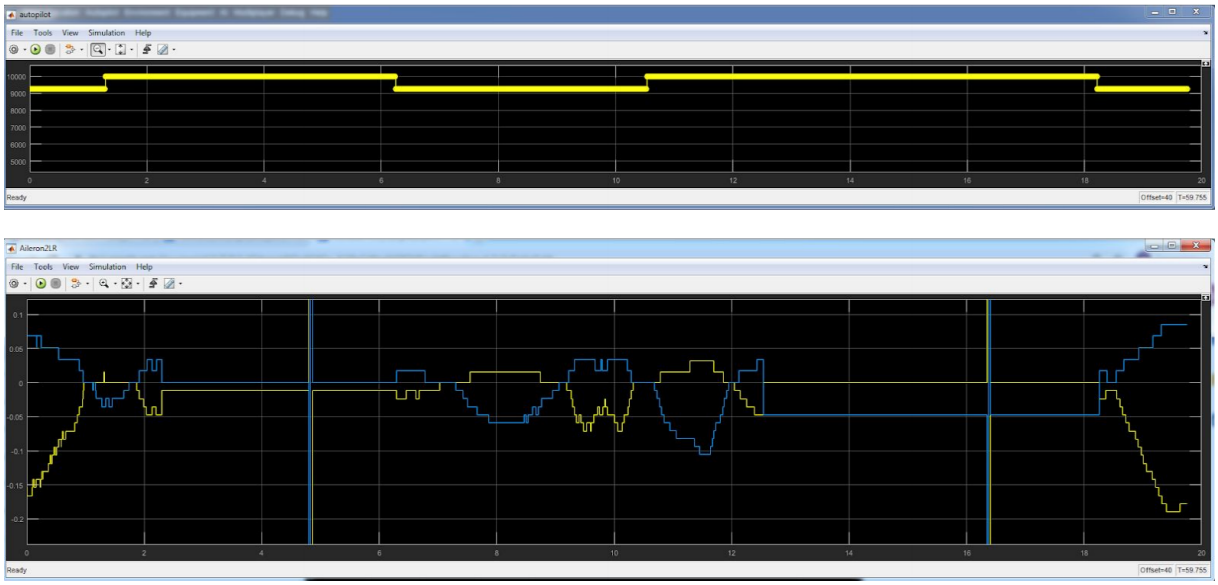

Figure 2.20 - Signal injection test in HIL

Ground tests on the demonstrator aircraft (SZTAKI)

For ground tests we prepared a test version of autopilot with only one difference compared to flight version: we gave a constant value for the controller instead of measured speed.

Augmented mode test:

1. Moved the aircraft to change pitch and roll
2. Control surfaces tried to stabilize the aircraft

Signal injection test:

1. Select initial velocity, amplitude multiplier and signal on mission planner (In RC AP1)
2. Inject the signal: switch to RC AP2
3. Related control surfaces moved according to the selected signal

Altitude and course angle test:

1. We gave altitude and course angle values via mavlink
2. Control surfaces tried to follow the given values

Autothrottle test:

1. We gave 38 m/s constant airspeed to the controller instead of measured value
2. Gave a velocity value via mavlink (in RC AP2)
3. The engine tried to increase or decrease the velocity depending on the given value

Table 1 shows the given commands and Figure 2.21 shows the response of the engine.

Switching times [sample]:	**Commanded velocity [m/s]:**
373000	38
378100	42
379900	38
385700	34
390700	42
393600	34
405000	38
406700	42
409100	34
415300	42
417700	38
420600	34
423800	38

Table 1 - The given velocity commands

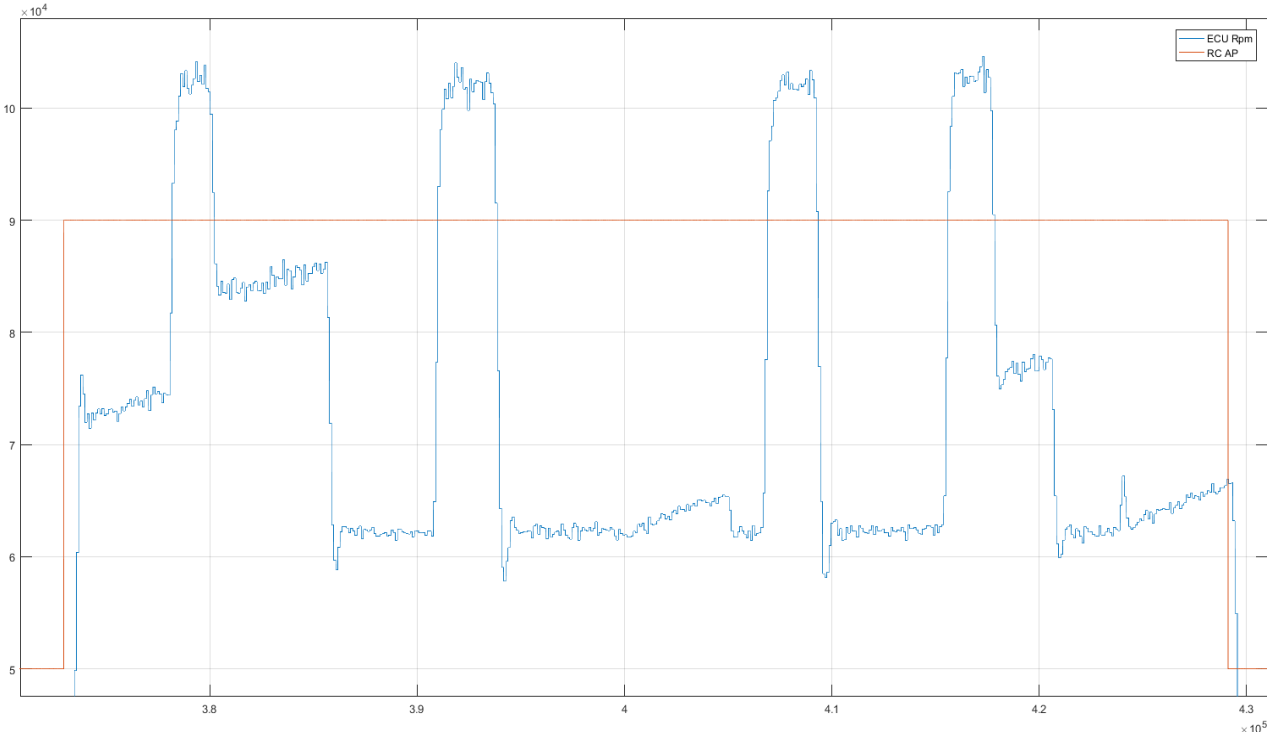

Figure 2.21 - Engine response for the given commands

Other preparations for flight test campaign (TUM)

As discussed during the winter months, operations of flight testing had to be streamlined. This resulted in going through all of the checklists and trying to find out, which checklist points could be reduced without reducing safety. Checklists for packing and system start-up were improved. Additional equipment like a radio for airport communication, printer and additional tool kit all helped to decrease the time required to set off for flight testing.

In addition to acquiring new equipment, another pilot has been trained to operate the FLEXOP demonstrator. This required multiple flights with a smaller jet turbine powered glider to be conducted. As a result, three pilots are now available for flight testing, increasing the overall redundancy and flexibility of the flight test crew. Also, another pilot and operator training session took place to restore the currency of the crew.

Figure 2.22. Third pilot preparing for training with a jet turbine sailplane.

In May it was decided to start planning the first flight test campaign. There were many uknowns still, due to landing gear not being fully fixed as well as uncertainty due to operational limitations imposed by Covid-19. In June, the first iterations of the landing gear were being tested, but the proper taxi test was only planned for the first day of the flight test campaign. Only the proper high-speed taxi test revealed that the solution applied did not give complete confidence to the pilots. Therefore for the next few days other solutions were being tested on the field, resulting in a need to postpone the actual flight test further to autumn. However, the flight planning was already finished for the first campaign and the test cards were fully prepared.

	Flight Test Card	Page II	Flight Test Programme: FLEXOP-FTP-01-00	
	1.9 Baseline Controller Check	Time	CN	Remarks

1.	Engine **ON**	FLEXOP ONE, FLEXOP TWO	*		
2.	REPORT READY FOR TAKE-OFF	MANAGER			
3.	CHECK CONTROLS, FULL DEFLECTIONS	FLEXOP ONE			
4.	JETI WARNINGS **ON**	FLEXOP ONE			
5.	BRAKES **ON**	FLEXOP 1, FLEXOP 2, OPERATOR, ENGINEER			
6.	STANDBY TO ANNOUNCE TAKE-OFF AT 18m/s	OPERATOR			
7.	THROTTLE 100%, BRAKES **OFF** WHEN AIRCRAFT MOVES	FLEXOP 1			T-0
8.	ANNOUNCE **V1**	MANAGER			T+7
9.	FLIGHT STATE CRUISE, THROTTLE 70%, CLIMB 200	FLEXOP 1			At 30 AGL
10.	TRIM 38m/s	FLEXOP 1			
11.	SWITCH AUTOPILOT 1	FLEXOP 1			

Figure 2.23. First page of the test cards, prepared for the upcoming flights.

Update and Validation of the -0 wing flight mechanical model (DLR-SR)

Structural Dynamics

The structural dynamics of a flexible aircraft can be divided into rigid body and flexible body dynamics. The rigid body dynamics basically describe the manoeuvre characteristics of the aircraft. In contrast, the flexible body dynamics represent the aircraft motion due to the flexibility of its structure. While the rigid body dynamics are described in nonlinear form, the equation of the flexible body dynamics is considered to be linear. A detailed FE model serves as basis for the structural model of the aircraft. The process of generating the FE model and its condensed version is described below. Subsequently, the EOM representing the rigid and flexible body dynamics are defined for the condensed model.

Finite Element Model

The aircraft structural FE model comprises the wing, fuselage and empennage and is shown in Figure 4. The FE software used here is MSC.NASTRAN. The wing is represented by a high-fidelity FE model comprising beam, surface and solid elements. Rigid body interpolation elements are added at predefined locations throughout the wing to facilitate the required model reduction. Further-more, the wing mass model is density-based as opposed to a lumped mass model. The fuselage structure is modelled using beam elements. The equivalent beam stiffnesses are obtained utilizing the cross sections of the fuselage hull at different sections and the lay-up of the hull. The mass is then lumped at the two beam nodes. The V-tail empennage FE model is shell-element-based comprising of the main structural load-bearing entities – the upper and lower skins, structural rubs, spars and the non-structural masses. Similar to the wing FE model, a density-based mass representation is used for the empennage as well.

Given that the FE model of the wing is of very high-fidelity (more than 600000 nodes), a Guyan reduction, also called condensation, is performed reducing the mass and stiffness matrix to less than 200 nodes in the condensed model.

Equations of Motion

The condensed model features rigid body and flexible modes, which are described by the EOM. These are based on an equilibrium of forces and moments. They describe the behaviour of the aircraft due to external loads originating from the aerodynamics and thrust. For simplification, the following assumptions are made.

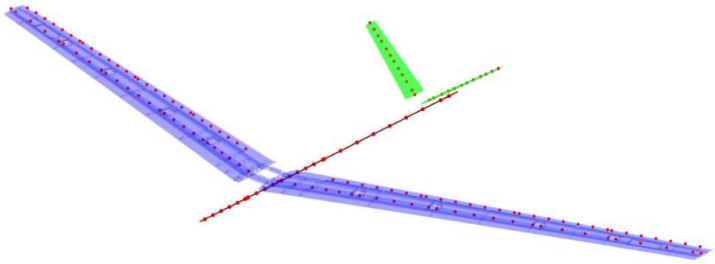

Figure 4: Full FE model of the FLEXOP demonstrator aircraft [9]

- As the earth rotation can be neglected, the inertial reference system is earth fixed.
- Gravity is constant over the airframe.
- The deformations of the airframe are considered to be small which allows the use of linear elastic theory defined by Hooke's law.
- Due to small deformations of the aircraft structure, the aircraft mass moment of inertia J_b remains unchanged.

- As the structural deformations are small, loads act on the undeformed airframe.
- The eigenvectors of the modal analysis are orthogonal, because of which the total structural deformation can be written as a linear combination of the modal deflections.
- The rigid body and flexible body EOM are considered to be decoupled.

Rigid Body Dynamics

For the derivation of the nonlinear flight mechanical EOM, the aircraft is considered as a rigid body with a constant mass m_b and constant mass moment of inertia J_b. Therefore, the aircraft rigid body motion is described by the Newton-Euler EOM

$$\begin{bmatrix} m_b(\dot{V}_b + \Omega_b \times V_b - T_{be} g_e) \\ J_b \dot{\Omega}_b + \Omega_b \times (J_b \Omega_b) \end{bmatrix} = \underbrace{\Phi_{gb}^T P_g^{\text{ext}}(t)}_{P_b^{\text{ext}}(t)} = \begin{bmatrix} F \\ M \end{bmatrix}, \quad (1)$$

In Equation (1) the translational and angular velocity of the aircraft with respect to the body frame of reference are given by V_b and $_b$. The vector g_e represents the gravitational acceleration, which is transformed with T_{be} from the earth-fixed to the body-fixed frame of reference. The external loads vector

$$P_g^{\text{ext}}(t) = P_g^{\text{eng}}(t) + P_g^{\text{aero}}(t) \qquad (2)$$

includes the loads acting on the aircraft structure. Here the loads due to the engine thrust $P_g^{eng}(t)$ and the aerodynamic loads $P_g^{aero}(t)$ are considered. By means of the matrix Φ_{gb}^T the external loads are transformed into the rigid body frame.

Flexible Body Dynamics

As the displacements due to the aircraft flexibility are assumed to be small, linear elastic theory is applied to define the flexible body motion. Therefore the correlation between external loads $P_g^{ext}(t)$ and the generalized coordinates u_f representing the modal deformation of the structure is given by the differential equation

$$M_{ff}\ddot{u}_f + B_{ff}\dot{u}_f + K_{ff}u_f = \underbrace{\Phi_{gf}^T P_g^{\text{ext}}(t)}_{P_f^{\text{ext}}(t)}. \qquad (3)$$

The matrices M_{ff} , B_{ff} and K_{ff} depict the modal masses, dampings and stiffnesses. The modal matrix $_{gf}$ contains the eigenvectors of the structural modes sorted by frequency. Typically, higher frequencies have a smaller contribution to the overall system performance. Consequently, modal truncation can be applied to reduce the DOF significantly by considering only the most relevant eigenmodes.

Aerodynamics

The aerodynamic loads represent the major external loads acting on the aircraft structure. Their calculation is based on the VLM for steady aerodynamics and the DLM for unsteady aerodynamics. Both methods are based on a panel model, which is described in the following section.

Panel Model

The lifting surfaces are discretised by several trapezoidal-shaped panels, known as aerodynamic boxes as shown in Figure 5. Of note is the panel model for the fuselage. The wetted areas of the fuselage are projected onto a T-cruciform shaped panel model. Although this is a vast simplification, the fuselage aerodynamics are modelled quite accurately with respect to higher-order CFD simulations.

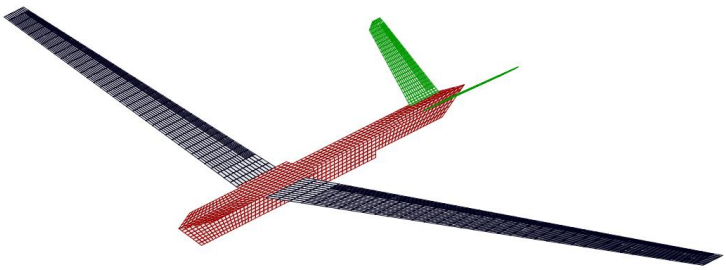

Figure 5: Aerodynamic boxes of the FLEXOP demonstrator aircraft [9]

Steady Aerodynamics— The VLM is used to model steady aerodynamics. As can be seen in Figure 6a, each aerody-

namic box of the panel model possesses a horseshoe vortex at point l on the quarter-chord line. Due to the Helmholtz theo-rem the vortex is shed downstream to infinity at the side edges of the box. For each aerodynamic box the Pistolesi Theorem needs to be met, stating that there is no perpendicular flow through the control point j at the three-quarter-chord line.

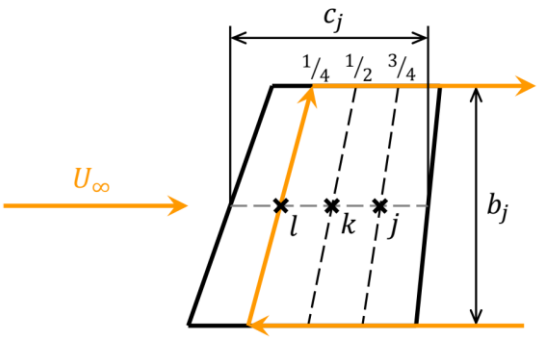

(a) Top view

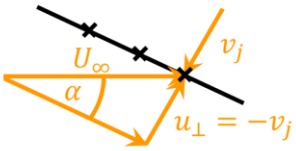

(b) Side view

Figure 6: Schematic drawing of an aerodynamic box [9]

Therefore the induced velocity at the control point needs to equalize the perpendicular component of the incoming flow, like shown in Figure 6b. By means of the Biot-Savart law the induced velocities v_j due to the circulation strengths $_j$ of the horseshoe vortices can be determined by

$$v_j = A_{jj}\Gamma_j. \tag{4}$$

The matrix A_{jj} describes the contribution of all vortices to the induced velocities of the aerodynamic boxes. Inverting A_{jj} and multiplying with $2=c_j$, where c_j is the chord length of the respective aerodynamic box, leads to the aerodynamic influence coefficient (AIC) matrix Q_{jj}. In the steady aerody-namic case it is considered constant. The pressure coefficient c_{pj} of a panel is then determined by

$$\Delta c_{pj} = Q_{jj} w_j, \tag{5}$$

where wj = is the velocity vj normalized with the flight speed U_∞. It is assumed to be equal to the angle of attack $_j$ of a panel, i.e. $w_j = \sin(w_j)$, as only small angles are considered. The downwash w_j comprises different aerodynamic contributions. It is affected by a rigid body motion of the aircraft

With

$$w_{jb_1} = \frac{c_r}{2U_\infty} D_{jk,2}\Phi_{ka}T_{ab}\begin{bmatrix} V_b \\ \Omega_b \end{bmatrix}. \tag{6}$$

The vector $[V_b^T\ \Omega_b^T]^T$ contains the rigid body velocities V_b and angular rates Ω_b and is transformed to the aerodynamic centre by means of T_{ab}. Subsequently, the respective motion of each panel reference point k is calculated by multiplying Φ_{ka} The resulting contribution to the downwash is then determined by

multiplication with the matrix $D_{jk;2}$ and factorisation with $c_r/2U_\infty$, where c_r depicts the reference chord length. Further details on the determination of the contributions of the downwash can be found in Ref. 10. Under the assumption of small angles Equation (6) can be rearranged to

$$\begin{aligned} w_{jb_1} &= \frac{c_r}{2} D_{jk,2} \Phi_{ka} \begin{bmatrix} \cos\alpha_a \cos\beta_a \\ \tan\beta_a \\ \sin\alpha_a \\ p_a/U_\infty \\ q_a/U_\infty \\ r_a/U_\infty \end{bmatrix} \\ &\approx \frac{c_r}{2} D_{jk,2} \Phi_{ka} \begin{bmatrix} 1 \\ \beta_a \\ \alpha_a \\ p_a/U_\infty \\ q_a/U_\infty \\ r_a/U_\infty \end{bmatrix}. \end{aligned} \tag{7}$$

It can be seen that, besides the angular rates p_a, q_a and r_a, the downwash is affected by the sideslip angle $_a$ and the angle of attack $_a$. The "1" in the vector represents a constant contribution to the downwash. This gives the opportunity to add the downwash caused by effects like camber and twist by adaptation of the first column of Φ_{ka}. As a first step, it is updated based on a steady computational fluid dynamics (CFD) calculation. The deflection of the control surfaces u_x is taken into account by changes in the downwash

$$w_{jx_0} = D_{jk,1} \Phi_{kx} u_x. \tag{8}$$

The matrix Φ_{ka} links control surface deflections to the corresponding aerodynamic boxes. The differentiation matrix $D_{jk,1}$ then relates a displacement of the panel reference point k to the downwash w_j. Besides, the control surface deflection rate alters the lift, which can be accounted for by

$$w_{jx_1} = \frac{c_r}{2U_\infty} D_{jk,2} \Phi_{kx} \dot{u}_x. \tag{9}$$

As depicted in Figure (3) the structural dynamics are affected by the aerodynamic loads P_g^{aero}. These can be expressed in terms of w_j as

$$P_g^{\text{aero}} = q_\infty T_{kg}^T S_{kj} Q_{jj} w_j + q_\infty T_{ag}^T S_r c_D, \tag{19}$$

where the second term represents the aerodynamic drag loads with reference area S_r and the transformation matrix from the mean aerodynamic centre to the structural grid T_{ag}^T. Matrix S_{kj} depicts an integration relating the pressure in the aerodynamic boxes at point j with the forces at the aerodynamic grid points k. The forces at the aerodynamic grid points k are then interpolated onto the structural grid points via the transpose of the spline matrix T_{kg}. The splining model of the wing is exemplary shown in Figure 7.

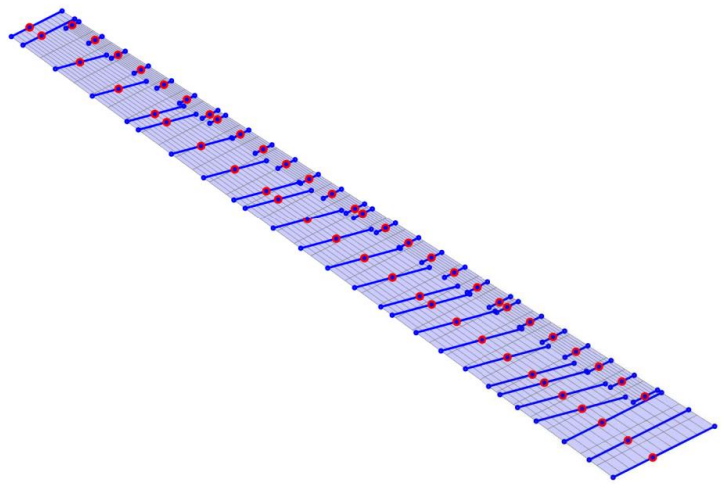

Figure 7: Splining between the aerodynamic model and structural model of the right wing [9]

Multiplying with the dynamic pressure q_∞ then leads to the aerodynamic loads acting on the structure. To distinguish between the distributions of the aerodynamic loads to the rigid and flexible body dynamics, Equation (19) is multiplied by Φ_{gb}^T and Φ_{gf}^T leading to

$$\begin{bmatrix} P_b^{\text{aero}} \\ P_f^{\text{aero}} \end{bmatrix} = \begin{bmatrix} \Phi_{gb}^T \\ \Phi_{gf}^T \end{bmatrix} P_g^{\text{aero}}. \qquad (20)$$

Due to aerodynamic loads the aircraft structure performs rigid body and flexible body motions which, in turn, affect the aircraft aerodynamics. Therefore the aeroelastic model is considered a loop between structural dynamics and aerodynamics.

Performed Manoeuvres

The parameter estimation process strongly depends on the performed manoeuvres in flight, as they define how well the characteristics of the aircraft can be determined. In order to define suitable excitation signals, a priori knowledge on the model is used. However, this is conflicting as the accuracy of the examined model determines the quality of the model parameters to be estimated. Nevertheless, under the assumption, that the chosen modelling process provides realistic results, this approach is considered applicable.

Flight Mechanical Manoeuvres

The first goal is to update the flight mechanical model. Therefore all contributions resulting from the aircraft flexibility are neglected. Besides, unsteady aerodynamic effects are ignored, as their contribution to the flight mechanical model is assumed to be small. As a result, for the aerodynamic load P_b^{aero} on the right-hand side of the rigid body equation of motion (1) it is only accounted for the downwash w_{jb1}, w_{jx0} and w_{jx1} yielding to

$$
\begin{aligned}
P_b^{\text{aero}} =& q_\infty \underbrace{\Phi_{gb}^T T_{kg}^T S_{kj} Q_{jj} \frac{c_r}{2} D_{jk,2} \Phi_{ka}}_{DQ_{h,b1}} \begin{bmatrix} 1 \\ \beta_a \\ \alpha_a \\ p_a/U_\infty \\ q_a/U_\infty \\ r_a/U_\infty \end{bmatrix} \\
&+ q_\infty \underbrace{\Phi_{gb}^T T_{kg}^T S_{kj} Q_{jj} D_{jk,1} \Phi_{kx}}_{DQ_{h,x0}} u_x \\
&+ q_\infty \underbrace{\Phi_{gb}^T T_{kg}^T S_{kj} Q_{jj} \frac{c_r}{2U_\infty} D_{jk,2} \Phi_{kx}}_{DQ_{h,x1}} \dot{u}_x .
\end{aligned} \tag{21}
$$

It is assumed, that the correlation between the control surfaces and the aerodynamic load given by the matrices DQ_{h,x_0} and DQ_{h,x_1} is accurately predicted by the proposed model. The focus is on an update of the rigid body contribution gathered in matrix DQ_{h,b_1}. It is a 6x6-matrix with the entries

$$
Dh_{b1} = \begin{bmatrix} 0 & 0 & 0 & 0 & 0 & 0 \\ 0 & f_{y\beta} & 0 & f_{yp} & 0 & f_{yr} \\ f_{z0} & 0 & f_{z\alpha} & 0 & f_{zq} & 0 \\ 0 & m_{x\beta} & 0 & m_{xp} & 0 & m_{xr} \\ m_{y0} & 0 & m_{y\alpha} & 0 & m_{yq} & 0 \\ 0 & m_{z\beta} & 0 & m_{zp} & 0 & m_{zr} \end{bmatrix} . \tag{22}
$$

There are 15 parameters, that are to be estimated. As can be seen the parameters related to forces in x-direction are neglected, due to the mentioned constraints of the model. Many more entries are equal to zero or considered too small to have a significant influence on the parameter estimation. The remaining parameters can be associated with either a longitudinal or a lateral aircraft motion.

In Table 2 the performed manoeuvres, separated in longitudinal and lateral, are listed with the parameters, that mainly contribute to the aircraft motion.

Table 2: Performed manoeuvres for the parameter estimation [11]

Longitudinal	
Steady level flight:	f_{z0}, $f_{z\alpha}$, m_{y0}, $m_{y\alpha}$
Pushover-pullup:	f_{z0}, $f_{z\alpha}$, f_{zq}
Short period:	$f_{z\alpha}$, f_{zq}, $m_{y\alpha}$, m_{yq}
Phugoid:	f_{z0}, $f_{z\alpha}$, f_{zq}, m_{y0}, $m_{y\alpha}$, m_{yq}
Lateral	
Steady sideslip:	$f_{y\beta}$, $m_{z\beta}$
Dutch-roll:	$f_{y\beta}$, f_{yr}, $m_{x\beta}$, m_{xr}, $m_{z\beta}$, m_{zr}
Bank-to-bank:	f_{yp}, m_{xp}, m_{zp}

The definition of the excitation signals for the short period, phugoid and dutch-roll mode are determined based on an a priori analysis of the initial model. The phugoid is excited by an elevator pulse, that is chosen to last 2 seconds with an amplitude of approximately 3°. This elevator deflection was found to

be appropriate to excite the phugoid mode of the aircraft. The dutch-roll mode can be excited by a doublet on the rudder. The amplitude is chosen to be around 3°, while the half time length $\Delta t_{doublet}$ of the doublet is calculated with the dutch-roll frequency $\omega_{dutch-roll}$ by the rule of thumb

$$\Delta t_{\text{doublet}} \approx \frac{2.3}{\omega_{\text{dutch-roll}}} \tag{23}$$

to be 1.22 seconds. The dutch-roll frequency $\omega_{dutch-roll}$ is determined from the simulation in advance of the flight test. Equivalently, the short period mode can be observed by exciting the elevator with a doublet. Equation (23) gives a $\Delta t_{doublet}$ of 0.24 seconds with the pre-determined frequency of the short-period $\omega_{short-period}$. The amplitude is chosen to be around 6°.

The steady level flight, pushover-pullup, steady sideslip and bank-to-bank manoeuvres were flown manually by the pilot.

Update of the Rigid Body Model

When it comes to updating an aircraft model or rather specific model parameters, a suitable process needs to be set up. On the one hand a model structure must be given including parameters to be estimated and on the other hand an optimization algorithm to find the somewhat best model parameters needs to be given. There exist different optimization algorithms to estimate model parameters, like the output error method (OEM), the filter error method (FEM) and more. Within the scope of this paper the output error method based on maximum likelihood estimation is chosen.

Output Error Method

In Figure 12 the basic procedure of the OEM is shown.

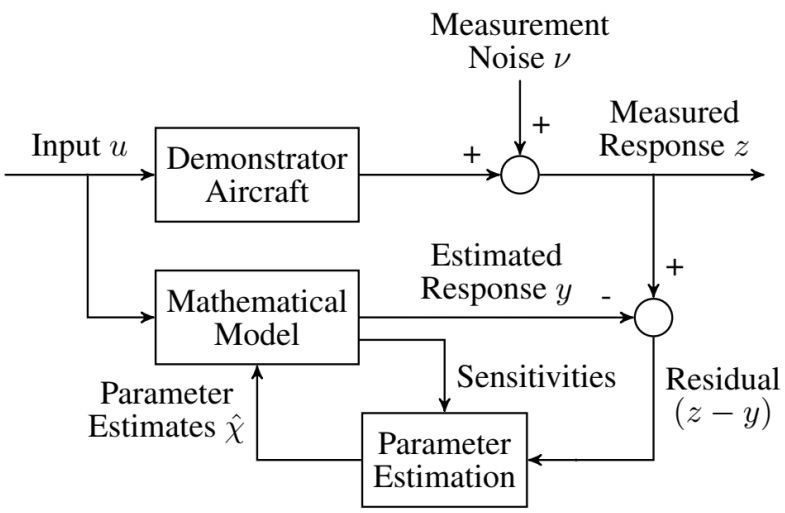

Figure 12: Concept of the output error method [25]

The upper path represents the flight test, where the outcome is the measured inputs and outputs. The OEM assumes, that the outputs are affected by measurement noise. Process noise, however, is neglected. Subsequently, the inputs are fed into the mathematical model to conduct a simulation of the considered flight test manoeuvre. Based on the difference between the flight test measurements and

the simulation outputs, the parameters of the mathematical model are updated by means of an optimisation.

It is assumed, that the model equations are given in the form of

$$\begin{aligned} \dot{x}(t) &= f(x(t), u(t), \chi),\ x(t_0) = x_0 \\ y(t) &= g(x(t), u(t), \chi) \\ z(t_k) &= y(t_k) + \nu(t_k). \end{aligned} \tag{24}$$

The first two equations describe the proposed mathematical model. They dependent on the desired parameters χ. The last equation provides the relation between the discrete flight test measurements z and the output of the measurement equation y at a time instant t_k. They exclusively differ in the measurement noise ν. The noise process is considered stochastic and is characterized by Gaussian white noise with zero mean. Its definition is

$$\begin{aligned} E\{\nu(t_k)\} &= 0 \\ E\{\nu(t_k)\nu(t_l)^T\} &= R\delta_{kl}. \end{aligned} \tag{25}$$

The second expression of Equation \ref{eq:gwn} suggests that the noise process white noise, as it is time independent. Simultaneously the amplitude depends on chance defined by a Gaussian distribution with covariance matrix R it describes Gaussian noise. As a result the measurement vector $z(t_k)$ with dimension n_z is affected by Gaussian white noise and therefore its values are assumed to be Gaussian distributed with a probability density function

$$\begin{aligned} p(z(t_k)|\chi) = &\frac{1}{(2\pi)^(n_z/2)sqrt|R|} \\ &\exp\left(-\frac{1}{2}(z(t_k) - y(t_k))^T R^{-1}(z(t_k) - y(t_k))\right). \end{aligned} \tag{26}$$

With respect to Equation (24) the expected value of $z(t_k)$ is assumed to be $E\{z(t_k)\} = y(t_k)$ for the model parameters χ. For a set of N measurements the likelihood function becomes

$$\begin{aligned} p(z(t_1), ..., z(t_N)|\chi) &= \prod_{k=1}^{N} p(z(t_k)|\chi) \\ &= [(2\pi)^{n_z}|R|]^{-N/2} \\ &\exp\left(-\frac{1}{2}\sum_{k=1}^{N}(z(t_k) - y(t_k))^T R^{-1}(z(t_k) - y(t_k))\right). \end{aligned} \tag{27}$$

Goal of the maximum likelihood method (MLM) is to identify the model parameters χ, which maximise the probability defined by Equation (27). The optimal solution is the maximum likelihood estimate obtained as

$$\begin{aligned}\hat{\chi}_{ML} &= \arg\left\{\max_{\chi} p(z|\chi)\right\} \\ &= \arg\left\{\min_{\chi}\left(-\ln p(z|\chi)\right)\right\}.\end{aligned} \tag{28}$$

For greater ease of handling the negative logarithm of the likelihood function $p(z|\chi)$ is considered, which simplifies Equation (27) to the cost function

$$\begin{aligned}J(\chi, R) =& \frac{1}{2}\sum_{k=1}^{N}\left((z(t_k) - y(t_k))^T R^{-1}(z(t_k) - y(t_k))\right) \\ &+ \frac{N}{2}\ln(|R|) + \frac{Nn_z}{2}\ln(2\pi).\end{aligned} \tag{29}$$

At this point it is assumed, that the covariance matrix R is unknown a priori. As R depends on the model parameters χ and vice versa, the relaxation strategy is used to find the optimal solution of the redefined likelihood function (29) in two steps. Firstly, for a given parameter vector χ the maximum likelihood estimate of R is obtained by setting the partial derivative $\partial J(\chi, R)/\partial R$\$ to zero. This yields

$$R = \frac{1}{N}\sum_{k=1}^{N}(z(t_k) - y(t_k))(z(t_k) - y(t_k))^T. \tag{30}$$

Secondly, substituting (30) in (29) provides

$$J(\chi) = \frac{1}{2}n_z N + \frac{N}{2}\ln(|R|) + \frac{Nn_z}{2}\ln(2\pi). \tag{31}$$

Apart from ln(|R|) all terms in Equation (31) are independent from the model parameters χ. The cost function therefore reduces to

$$J(\chi) = \det(R). \tag{32}$$

Equation (32) is solved iteratively for the optimal model parameter χ by means of a Gauss-Newton algorithm.

Two-Step Method

By means of the two-step method (TSM) the model parameters can be determined. The TSM divides the state and parameter estimation problem in a flight path reconstruction and a parameter identification part. The flight path reconstruction is used to accurately reconstruct the time history of the aircraft states during the manoeuvre and besides allows the determination of potential instrumentation errors. As some sensor readings, like the angle of attack and the airspeed, are prone to be inaccurate, the measurements are improved based on past, present and future data and the flight mechanical equations. Subsequently, the identification of the model parameters follows.

The success of the TSM depends on the aircraft to be tested, the aircraft instrumentation, the excitation signals, the mathematical model selected for identification and the chosen algorithm for the analysis and adaption of the model.

Flight Path Reconstruction

The flight path reconstruction is based on a non-linear state-space system consisting of flight mechanical state and measurement equations. The considered inputs are the translational accelerations a_{bm} and the rotational rates Ω_{bm} measured in flight by an IMU placed in the fuselage. The states are the velocity vector V_b, the Euler angles ϕ, θ and ψ and the altitude h. The resulting state equations are given by

$$\dot{V}_b = a_b - (\Omega_{b,m} - \Delta\Omega_b) \times V_b + T_{be} g_e \tag{33}$$

$$\begin{bmatrix} \dot{\phi} \\ \dot{\theta} \\ \dot{\psi} \end{bmatrix} = \begin{bmatrix} 1 & \sin\phi\tan\theta & \cos\phi\tan\theta \\ 0 & \cos\phi & -\sin\phi \\ 0 & \frac{\sin\phi}{\sin\theta} & \frac{\cos\phi}{\sin\theta} \end{bmatrix} (\Omega_{b,m} - \Delta\Omega_b) \tag{34}$$

$$\dot{h} = \begin{bmatrix} 0 & 0 & -1 \end{bmatrix} T_{be}^{-1} V_b. \tag{35}$$

Starting point of the state equations is the equilibrium of forces of the rigid-body equation of motion. Solving Equation (1) for $\dot{V}_b$ leads to Equation (33), where Ω_b is replaced by its flight test measurement Ω_{bm} including a potential sensor bias $\Delta\Omega_b$. The translational acceleration a_b is given with respect to the center of gravity. It is determined by

$$a_b = a_{b,m} - \dot{\Omega}_b \times d_s - \Omega_b \times (\Omega_b \times d_s) - \Delta a_b. \tag{36}$$

The acceleration measurement $a_{b,m}$ needs to be corrected for the coriolis and the centrifugal force caused by the offset between the acceleration sensor position and the center of gravity d_s. A potential sensor bias is covered by Δa_b. Additional state equations of the Euler angles ϕ, θ and ψ are considered through Equation (34). The remaining state equation is given by Equation (35). The inverse of T_{be} transforms the velocity V_b to the Earth-fixed frame of reference. Extracting only the element, which contributes to the z-direction, and changing the sign leads to the derivative of the altitude $\dot{h}$.

The outputs or reconstructed instrumentation measurements are the true airspeed $U_{\infty,r}$, the angle of attack α_r, the sideslip angle β_r, the Euler angles ϕ_r, θ_r and ψ_r and the altitude h_r. The corresponding measurement equations are given by

$$U_{\infty,r} = \|V_b\|_2 \tag{37}$$

$$\alpha_r = K_\alpha \tan^{-1}\left(\frac{V_{nb,z}}{V_{nb,x}}\right) + \Delta\alpha \tag{38}$$

$$\beta_r = K_\beta \sin^{-1}\left(\frac{V_{nb,y}}{|V_{nb}|}\right) + \Delta\beta \tag{39}$$

$$\phi_r = \phi \tag{40}$$

$$\theta_r = \theta \tag{41}$$

$$\psi_r = \psi \tag{42}$$

$$h_r = h. \tag{43}$$

As the α and β measurements of the noseboom are sensitive to errors, the scaling and bias variables K_α, $\Delta\alpha$, K_β and $\Delta\beta$ are introduced. The velocity vector V_{nb} at the noseboom is determined by

$$V_{nb} = V_b + (\Omega_{b,m} - \Delta\Omega_b) \times d_{nb}, \tag{44}$$

where d_{nb} is the distance between the aircraft CG and the noseboom. In theory the difference between the flight test measurements and the reconstructed measurements in (37)-(43) with respect to the OEM is only coming from the process noise ν.

The unknown parameters $\Delta\Omega_b$, Δa_b, K_α, $\Delta\alpha$, K_β, $\Delta\beta$ as well as the initial states V_{b0}, $[\phi_0\ \theta_0\ \psi_0]^T$, h_0 in Equations (33)-(35) are determined based on the introduced OEM algorithm. The residual (z-y) to be minimized is the difference between the flight test measurements and their reconstructed counterpart in Equations (37)-(43).

The FPR is performed for each considered manoeuvre type separately. Figures 13 and 14 depict the FPR exemplary for a pushover-pullup manoeuvre (POPU) and for a sideslip manoeuvre (SL) in comparison with the measured flight test data (FTD).

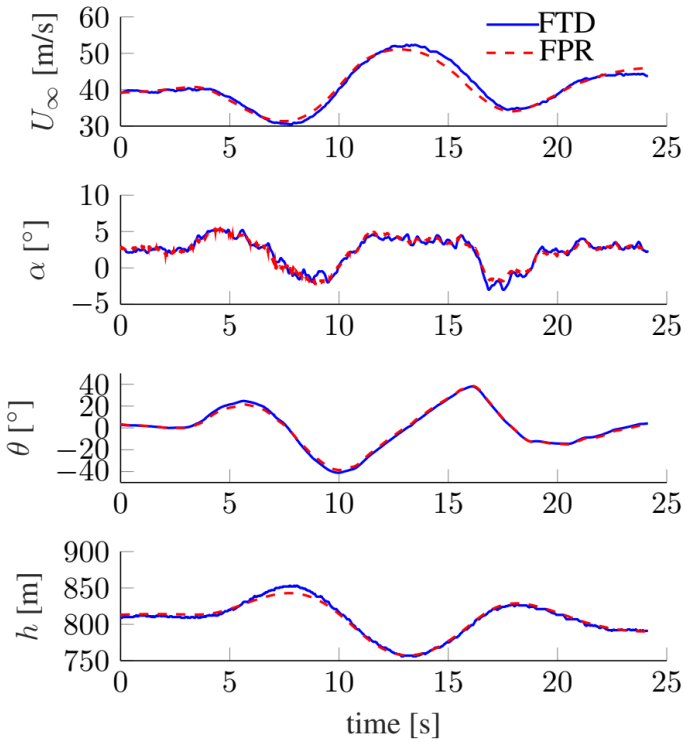

Figure 13: Comparison of reconstructed and flight test measurements (POPU)

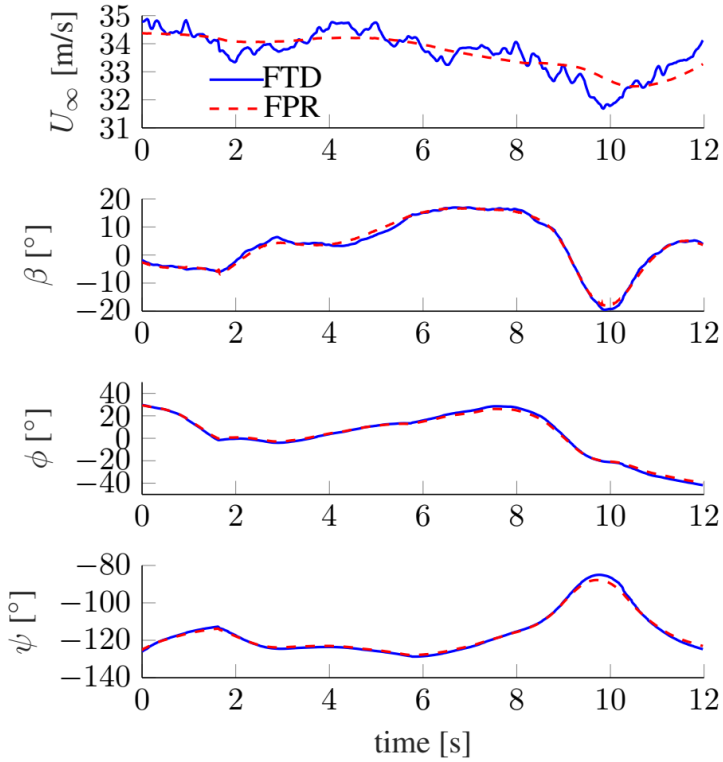

Figure 14: Comparison of reconstructed and flight test measurements (SL)

Only the measurement variables that play a major role for the manoeuvres are shown. For the POPU manoeuvre it can be seen, that α changes dynamically, while the remaining measurements are rather smooth. Nevertheless, the reconstructed α follows very closely the measurement.

The sideslip manoeuvre is not performed at a constant β as intended. However, it still offers the opportunity for updating lateral model parameters. The FPR follows the trends of the observations very well. An exception is the reconstructed true airspeed U_∞ which follows the trend of the measurement, but does not change as dynamically. As this behaviour is not observed for the additional measurements, it is valid to say the true airspeed is more strongly affected by disturbance.

Parameter Estimation

The parameter estimation is the second step of the two step method. The control surface deflections commanded during the various flight test manoeuvres are fed in the rigid body equation of motion (1). As mentioned before the parameters of the matrix $DQ_{h,b1}$ defined in Equation (21) are to be estimated. Based on the comparison between the outputs of the flight test z and the simulation y the model parameters are updated like described in the section “Output Error Method”.

The parameters corresponding to the longitudinal and lateral motion respectively are updated in separate steps. At first, the lateral manoeuvres are used to improve the matrix $DQ_{h,b1}$ with respect to the parameters $f_{y\beta}$, f_{yp}, f_{yr}, $m_{x\beta}$, m_{xp}, m_{xr}, $m_{z\beta}$, m_{zp} and m_{zr}. Subsequently, the longitudinal parameters f_{z0}, $f_{z\alpha}$, f_{zq}, m_{y0}, $m_{y\alpha}$ and m_{yq} are updated with the matrix $DQ_{h,b1}$ coming from the previous step. The final step is to redo the lateral update. This approach is chosen, because the longitudinal

manoeuvres also feature lateral contributions and vice versa. Therefore, a strict separation of the manoeuvres is not possible.

At the end, the OEM leads to the parameters summarized in Tables (3) and (4).

Table 3: Initial and final longitudinal parameters

Parameter	Initial	Final
f_{z0}:	-0.601	-0.484
$f_{z\alpha}$:	-15.12	-15.19
f_{zq}:	-7.41	-0.056
m_{y0}:	0.067	-0.02
$m_{y\alpha}$:	-1.63	-2.19
m_{yq}:	-13.58	-5.94

Table 4: Initial and final lateral parameters

Parameter	Initial	Final
$f_{y\beta}$:	-0.621	-0.661
f_{yp}:	-0.321	-2.35
f_{yr}:	2.52	3.41
$m_{x\beta}$:	-0.382	-2.08
m_{xp}:	-109.9	-126.4
m_{xr}:	1.28	32.61
$m_{z\beta}$:	0.464	0.48
m_{zp}:	0.294	-3.95
m_{zr}:	-4.02	-4.05

Of note is that the f_{z0} contributing to the lift with respect to camber and drag was lightly overestimated with the CFD calculations mentioned before. For corresponding moment coefficient m_{y0}, however, undergoes a relatively big change and switches sign. The $f_{z\alpha}$ and $f_{y\beta}$ value does not change much, which proves the strength of the VLM/DLM modelling approach. Some final parameter values differ strongly from their initial values. It is still under investigation to what extent the simplified modelling of the x-forces plays a role.

When the pushover-pullup (POPU) manoeuvre is performed with the model featuring the estimated parameters (PE), one can recognize a strong similarity with the reconstructed flight test data (FPR). Figure 15 depicts the trend of some of the observation variables affected by a longitudinal motion.

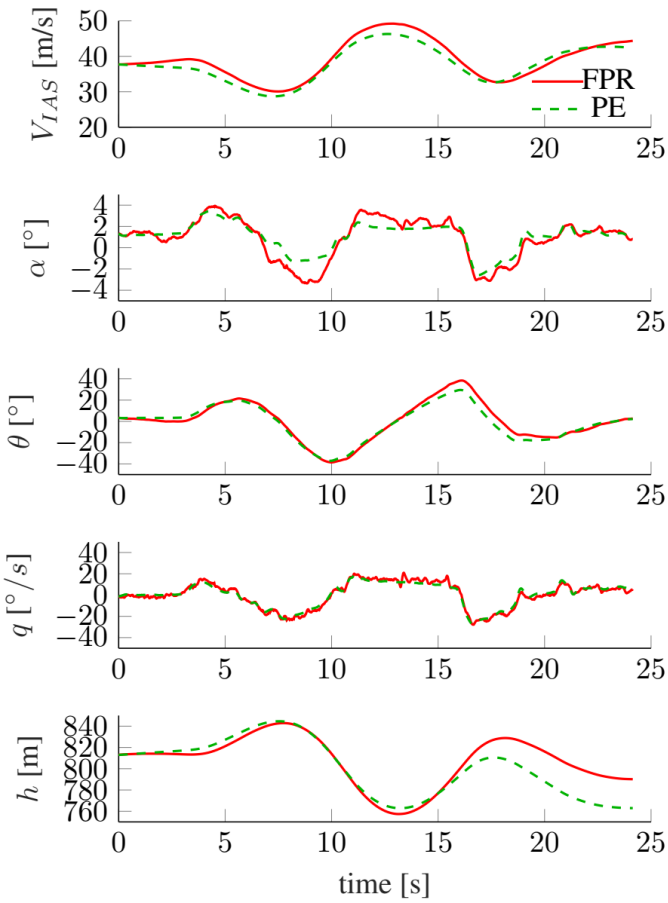

Figure 15: Comparison between reconstructed and simulated measurements (POPU)

The difference between the reconstructed and simulated angle of attack α possibly reveals the sensitivity to external disturbances. However, especially the pitch rate q matches very well between both data sets.

The measurements of the sideslip manoeuvre exhibited in Figure 16 proves, that the set of estimated parameters of the model fits well with the flight test data.

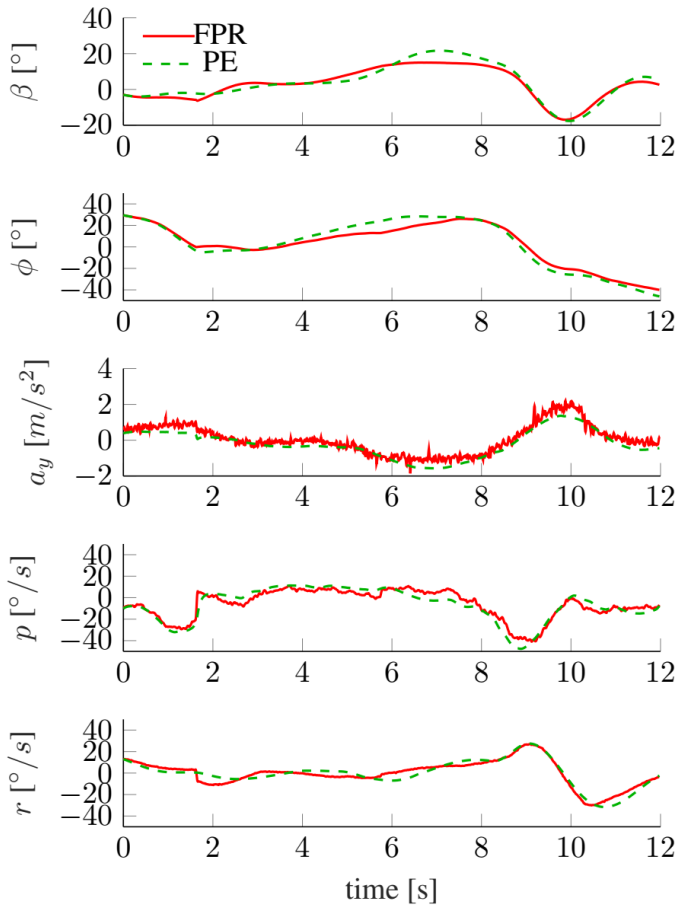

Figure 16: Comparison between reconstructed and simulated measurements (SL)

2.3.4 Deviations, their reason, impact on the project and corrective actions

The biggest deviation came from not being able to fix the aircraft's ground controllability in a timely manner. This mainly was due to two reasons: there were restrictions imposed on access to the workshops at TUM and the problem appeared to be way more difficult to solve than was initially anticipated. The many iterations, implementation of which only started in June, could only help bit by bit. In addition, not having a workshop at the airport, this proved time-costly to try new concepts out.

Due to the landing gear problems, it was decided not to risk the aircraft and not attempt to conduct test flights as was planned before. Therefore, the first flight test campaign had to be postponed to later on in autumn.

Figure 2.24. Another close call due to the inadequate steering on the ground. The demonstrator stopped shortly before the taxiway lamp.

2.4 Explanation of the work carried per WP- Work Package 4

2.4.1 Objectives and activities

Demonstrate applicability of the collaborative design process to a (full-scale) passenger aircraft

Quantify benefits of integrated aircraft and controls design in terms of structural weight reduction and aircraft over-all performance parameters

2.4.2 Starting point and approach

WP4 will start at M18, so only preparatory tasks have been completed related to the scale-up activities.

2.4.3 Efforts and achieved results, name involved contractors

The whole consortium, with the lead of DLR-AE and DLR-SR

The D150 configuration was developed within the DLR project VAMP [1]. It is comparable to the Airbus A320-200. Data published by the manufacturer, for example on the Airbus website, and input data to the preliminary design program PrADO for the application example Airbus A320, are used for the D150 configuration [2]. Its geometry is shown in Figure 1.

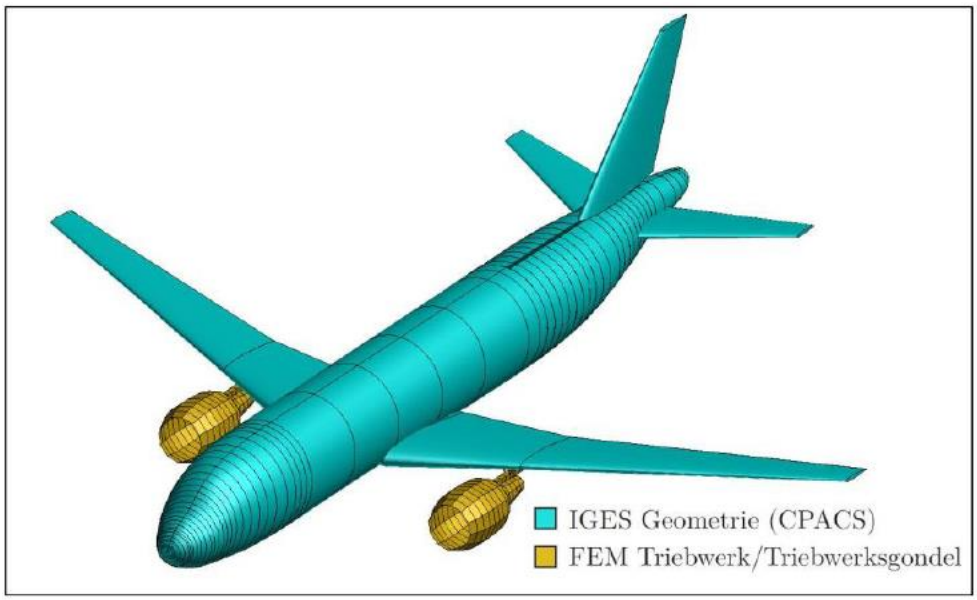

Figure 2.25 IGES-geometry of the D150 configuration

I have drafted the following as the project's requirements of the model.

Please edit or add to this email so that I could discuss and confirm with those familiar, that the model is suited to our needs.

The following are our requirements of the model.

1. Aircraft model available in a CPACS dataset (primarily, information necessary to generate FE+DLM model of the aircraft – fuselage, wings, HTP (horizontal tail-plane)/VTP (vertical tail-plane), interfaces, masses-system+payload+fuel)
2. NASTRAN FE+DLM model generated using the CPACS dataset with ModGen
3. Parametric FE+DLM model generation of wings and HTP possible
4. Parameter changes envisioned via CPACS for wing and HTP – planform (airfoil positions, chord, span), jig twist, position of spars, number and position of ribs, number and position of control surfaces, system masses (actuators, control surfaces) – for the HTP, only a subset of the above
5. FE model type – GFEM/Dynamic suited for structural dynamics (SOL103) and aeroelastic analysis (SOL144, SOL145)
6. Wing FE model will be used for structural optimization (HTP will be optimized as well?)

The following are NOT planned requirements of the model.

1. CFD simulations (details as such belly fairings are not modelled – IGES surfaces of individual entities such as wing, HTP, VTP are available)
2. Internal structure of fuselage - beam model of the fuselage sufficient for structural dynamic analyses (is a rigid fuselage okay for our purposes?)
3. Structural FE elements of the control surfaces + associated kinematics (control surfaces included only as aerodynamic panels in the DLM model)
4. FE models generated for the purpose of detailed/stress analyses
5. Availability of CAD model of the full aircraft
6. Information proprietary to other institutes in the CPACS dataset (can be preferably removed) – only information pertaining to our requirements is needed and is to be detailed

2.4.4 Deviations, their reason, impact on the project and corrective actions

Since WP4 have not started yet no corrective action have been implemented due to deviations.

2.5 Explanation of the work carried per WP- Work Package 5

2.5.1 Objectives and activities

• Project Coordination

• Evaluation of collaborative tools and their best practices

• Management of exploitation and dissemination of project results

2.5.2 Starting point and approach

The consortium is made up of four beneficiaries. Three of them (SZTAKI, TUM, DLR) have been involved in our previous coordinated project (FLEXOP) and with the fourth one (ONERA) we have had several common H2020 projects already (VISION). The previous cooperations imply a smooth project implementation on the management side.

2.5.3 Efforts and achieved results, name involved contractors

Task 5.1: Project Management (SZTAKI)

The main activities of the Management Team were:

• Ensured achievements of overall project schedule and objectives by

o Constant monitoring of project achievements against the work plan – there was a notable delay in project implementation due to the outbreak of Covid-19 epidemics (see section Deviations, their reason, impact on the project and corrective actions)

o Identification of risks and definition of risk mitigation measures through the Risk Reigster

o Solving any technical, financial, administrative or contractual issues or conflicts between partners, when needed

• Handled and distributed the funds according to the rules agreed within the consortium – pre-financing was distributed according to the Consortium Agreement.

1	SZTAKI	800 156,25
2	TUM	926 531,25
3	DLR	706 121,25
4	ONERA	451 875,00

• Maintained regular contact with the partner organisations

• Established a scientific and industrial advisory group

The Scientific Advisory Group (SAG) was confirmed by the Steering Committe in the first month of the Project for the purpose of offering advice and support on a wide range of Project-relevant issues. Members of the SAG shall be internationally recognised experts in the field of the Project.

Prof. Peter Seiler, Faculty of Electrical Engineering & Computer Science, University of Michigan
Daniel Ossmann from Munich University of Applied Sciences
Roeland de Breuker from Technical University of Delft.

The Industrial Advisory Group (IAG) includes key experts from the FLiPASED domains representing the key OEMs from Europe. Members were confirmed by the Steering Committe in the first month of the Project

Sebastien Blanc A350XWB loads and aeroelastics Designated Expert and Airbus - Active Adaptive Wing Leader, Airbus Commercial Aircraft
Carlo Aquilini, Airbus Defence and Space
Colo Ludovic (Aero-Structural design directorate) From Dassult- Aviation
Olivier Cantinaud (Technical Systems Directorate, Flight Dynamics Department) From DassultAviation

• Managed risk and settle any disputes within the consortium

• Organised the management team meetings, consortium meetings and meetings with scientific advisory group

Kick-off meeting: of the project has taken place at (and hosted by) SZTAKI on 12-13th September 2020. All 4 of the partners and the members of the Scientific and the Industrial Advisory Group got together for the first time. The meeting started with presentations of each partner and followed by project presentations. Steering committee meeting was also held where the members of the Management Support Team and the Scientific and the Industrial Advisory Group as well as the WP Leaders were elected.

1st Progress Meeting: of the project was planned to be held on the 19-20th of March in Münich but is was postponed and replaced by several thematic (and WP specialized) online meetings due to the emerging COVID situation.

weekly webexes were held by the coordinator – usually dedicated to a WP or a relevant deliverable – 21 meetings until the end of August.

WP/deliverable webexes were also organized by the coordinator or by different partner organisations whenever needed by the workflow – 8 meetings dedicated to Fligt Testing (3), D1.2 Toolchain workshop, bubt also to Flutter Evasive Action and MDO.

See the meeting folder with relevant presentations and minutes

https://dms.sztaki.hu/nextcloud/s/s8n79K4HJPMTQbp

• Reported to and chaired steering committee on the consortium meetings

• Reviewed and validated the project reports to ensure consistency with the project tasks (especially in the case of reviewing the different project implementation concepts and deliverables)

• Submitted reports and other deliverables to the Commission – 4 deliverables submitted (for the rescheduling of the project please see section 6Deviations from Annex 1

• Transmitted documents and information connected with the Project to and between the WorkPackage Leaders and the partner concerned

• Prepared and updated the schedules of the whole project (for the rescheduling of the project please see section 6Deviations from Annex 1

• Ethical, social and gender issues encountered during the project life will be monitored. It includes activities for preparing the gender issues plan and support to the other partners for applying the plan. (During Grant Preparation phase a separate deliverable was introduced to the project in a new WP called EPQ - Requirement No. 1 – the deliverable is ebing elaborated at the moment)

A Project Handbook defining procedures, templates and methods for the assessment of project achievements was issued in the beginning of the project. It was also submitted as a deliverable.

Every 12 months a progress report on project level will be issued, indicating the status of the project. This deliverable is the first one among the progress reports.

The organisation of the workshops with the scientific advisory group will be financially supported.

The travel expenses of the scientific advisory group are financially covered by WP5 – their participation on the Kick-off meeting was already paid by WP5 (coordinator).

Task 5.2: Collaboration tools, methods and practices (SZTAKI)

Common problem in multidisciplinary projects is the lack of understanding between partners due to their background and expertise, which leads to conservative designs or creates miscommunication, risking delays, costly re-designs or redundant solutions for the same problem by multiple stakeholders. We planned to tackle these issues by implementing collaborative project management solutions. After a thorough analysis of the different workflows and work groups we decided to use the following tools: Nextcloud for sharing, editing documents, defining tasks. Webex for online meetings. overleaf and GIT.

Task 5.3: Exploitation and Dissemination Management (SZTAKI)

This task includes:

• Observation of the evolving research and development trends as well as communication of the observances to the consortium members – follow-up done by the coordinator.

• Co-ordination of issues related to Intellectual Property Rights – this topic is regulated in the Consortium Agreement the partners have signed.

• Set-up of an Exploitation and Dissemination Plan; dissemination of results will be achieved by publications of individual partners. Furthermore a session organised in the most appropriate international congress will be organised to give a survey of the achievements within the project.

Several publications have already been submitted by project partners (see in section Scientific publications). The Exploitation and Dissemintation Plan is to be set up by the 31st of August 2021.

• In accordance with the dissemination plan the consortium members have to identify results with potential for patenting and publication activities must be aligned with patent application rules – this topic is regulated in the Consortium Agreement the partners have signed.

2.5.4 Deviations, their reason, impact on the project and corrective actions

See section Deviations from Annex 1

Table 5: Summary of meetings organised for all Work Packages in this reporting period

Name	Partner organising	Particiapating Partners	Link for Minutes of Meeting	Date
Flight Test Workshop I	TUM	SZTAKI, DLR, ONERA		26.03.2020
Flight Test Workshop II	TUM	SZTAKI, DLR, ONERA		31.03.2020
Emergency Flutter Action	TUM	SZTAKI, DLR		08.04.2020
Flight Test Workshop III	TUM	SZTAKI, DLR, ONERA		12.05.2020
Software and hardware updates on the aircraft	TUM	SZTAKI		20-24.07.2020

2.6 Impact

The impact of the project, leading to improved design environment and more streamlined interfaces between disciplinary functions remains highly relevant. Both Airbus and Boeing devoted significant effort into this area via the Airbus – University of Michigan collaboration and via the Boeing Loyal Wingman program where digital twins and simulation-based flight testing is utilized.

Specific impacts are still expected in the following areas:

- *Advanced multidisciplinary and collaborative capabilities for whole aircraft along its life cycle. – The* collaborative multi-disciplinary aspects are highly targeted by the work and the corresponding deliverables of the consortium, these will lead to enhanced design, demonstration and scale-up.
- *Significantly reduced aircraft design cycle and higher complexity decision trade-offs.* – The consortium already tackled many of the interdisciplinary hurdles of taking structures, control and aircraft overall design into the same MDO loop, the tools are not working in one overall optimization yet, but common interfaces have been set-up, and the benefits of taking less compromises during a/c design are more clear for the partners.
- *Development of synergies on visualisation methods and big-data analytics.* - The collaboration among prominent Research Institutes and Universities with the large amount of generated data already fueled further collaboration beyond the consortium, for example with SUPAERO and University of Michigan.
- *Increase the European innovation potential in Aeronautics and Air Transport (AAT) by a more balanced and integrated collaboration of industry, including SMEs and research providers*. - The developed tools and methods will aim at standardizing the interfaces between teams, which will have great impact on the possibilities of collaboration between industry, academia and SMEs.

3 Update of the plan for exploitation and dissemination of result plan (Technical Report 2)

Not Applicable - Exploitation and Dissemination Plan is due in M24.

4 Update of the data management plan (if applicable)

Not Applicable – first version of Data Management Plan was submitted in this period.

5 Follow-up of recommendations and comments from previous review(s) (if applicable)

Not applicable – no project reviews have been conducted in the first 12 months of the project.

6 Deviations from Annex 1

6.1 Tasks

The project started on 1st of September 2019 and the consortium members gathered on the 12 and 13 of September in Budapest for the kick-off meeting. Since then, the works have been running on two fronts:

- Conducting experiments to support our flight test campaign
- Develop a multidisciplinary design optimization (MDO) toolchain for aircraft conceptual design where control design tasks as well as aerodynamics and structure related parameters are optimised in parallel

Since the kick-off meeting, 8 dedicated webex sessions were organized on specific related topics: toolchain, flight test, MDOand 23 weekly regular status report teleconferences were held. Moreover, SZTAKI visited TUM for a week (20-24 of July) to mature the onboard avionics system in preparation for the flight test. TUM planned to conduct flight test first in the last week of July, followed by the first week of August. Multiple taxi tests at EDMO airfield were conducted with the fully instrumented demonstrator, but due to ground controllability issues the demonstrator did not get airborne. A plan is in place to change the landing gear configuration and resume flight testing.

The flight-testing campaign was interrupted by a damage to the demonstrator at EDMO airfield, where the aircraft hit a runway light during high speed taxi testing. Its wing suffered minor damage, what was fixed within a week. Due to this incident, it was decided that the landing gear arrangement has to be redesigned to improve ground handling, otherwise the risk of subsequent collisions might be too high. It already took 2 months to fix, and we plan to conduct the next high-speed taxi test on the first week of October, 2020. In case the changes are not sufficient the complete landing gear has to be replaced, which involves modifications on the fuselage, what might take another 4 months from now.

The overall project is behind schedule, what is currently estimated to be 3 months on the flight-testing side and 3.5 months on the MDO workflow side. This is due to the lack of face to face meetings (both internally and consortium wide) since DLR is working from home office for the last 6 months, ONERA reduced the workload for employees for 4 weeks only to 24 hours a week, and mandated home office for another 3 months. Home office at TUM also lasted 4 months, while access to laboratories were severely restricted. SZTAKI also mandated home office for 2.5 months, when employees used laboratory equipment at home to continue with their work. Laboratory work and manufacturing / integration was not possible for the partners for 3 months.

GANTT chart

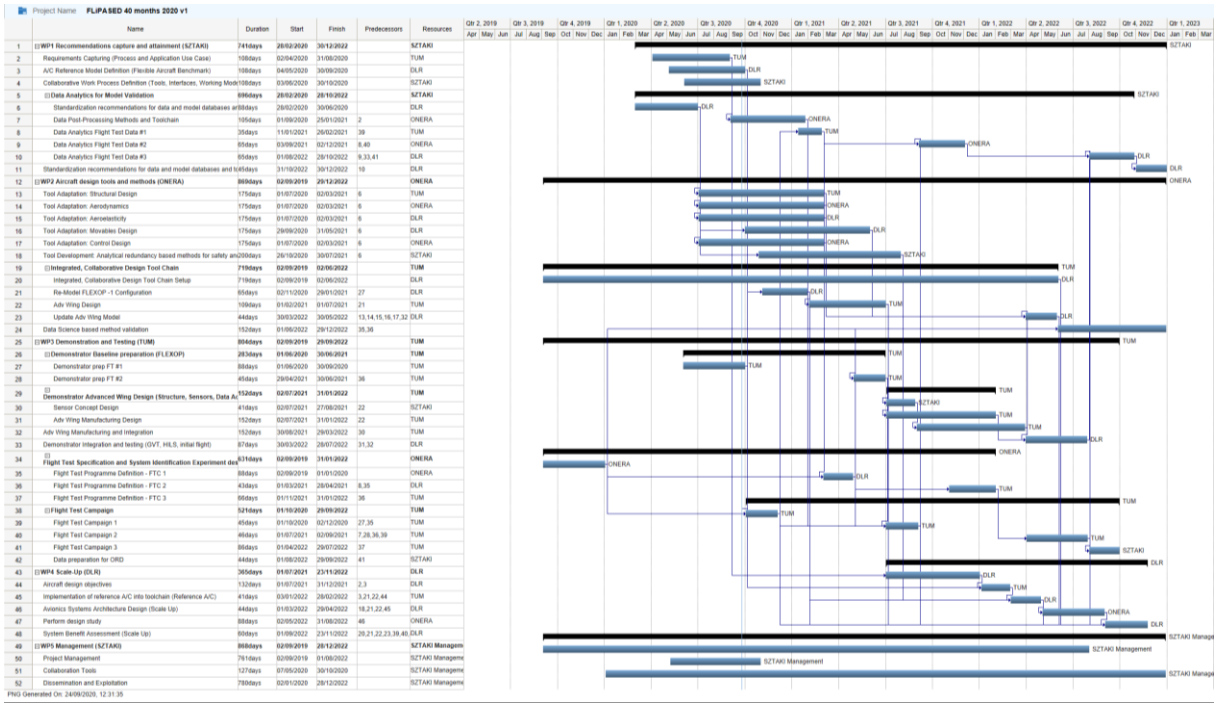

Project Name FLIPASED 40 months 2020 v1

	Name	Duration	Start	Finish	Predecessors	Resources
1	WP1 Recommendations capture and attainment (SZTAKI)	741days	28/02/2020	30/12/2022		SZTAKI
2	Requirements Capturing (Process and Application Use Case)	108days	02/04/2020	31/08/2020		TUM
3	A/C Reference Model Definition (Flexible Aircraft Benchmark)	108days	04/05/2020	30/09/2020		DLR
4	Collaborative Work Process Definition (Tools, Interfaces, Working Mode	108days	03/06/2020	30/10/2020		SZTAKI
5	Data Analytics for Model Validation	896days	28/02/2020	28/10/2022		SZTAKI
6	Standardization recommendations for data and model databases ar	88days	28/02/2020	30/06/2020		DLR
7	Data Post-Processing Methods and Toolchain	105days	01/09/2020	25/01/2021	2	ONERA
8	Data Analytics Flight Test Data #1	35days	11/01/2021	26/02/2021	39	TUM
9	Data Analytics Flight Test Data #2	65days	03/09/2021	02/12/2021	8,40	ONERA
10	Data Analytics Flight Test Data #3	65days	01/08/2022	28/10/2022	9,33,41	DLR
11	Standardization recommendations for data and model databases and to	65days	31/10/2022	30/12/2022	10	DLR
12	WP2 Aircraft design tools and methods (ONERA)	869days	02/09/2019	29/12/2022		ONERA
13	Tool Adaptation: Structural Design	175days	01/07/2020	02/03/2021	6	TUM
14	Tool Adaptation: Aerodynamics	175days	01/07/2020	02/03/2021	6	ONERA
15	Tool Adaptation: Aeroelasticity	175days	01/07/2020	02/03/2021	6	DLR
16	Tool Adaptation: Movables Design	175days	29/09/2020	31/05/2021	6	DLR
17	Tool Adaptation: Control Design	175days	01/07/2020	02/03/2021	6	ONERA
18	Tool Development: Analytical redundancy based methods for safety an	200days	26/10/2020	30/07/2021	6	SZTAKI
19	Integrated, Collaborative Design Tool Chain	719days	02/09/2019	02/06/2022		TUM
20	Integrated, Collaborative Design Tool Chain Setup	719days	02/09/2019	02/06/2022		DLR
21	Re-Model FLEXOP -1 Configuration	65days	02/11/2020	29/01/2021	27	DLR
22	Adv Wing Design	109days	01/02/2021	01/07/2021	21	TUM
23	Update Adv Wing Model	44days	30/03/2022	30/05/2022	13,14,15,16,17,32	DLR
24	Data Science based method validation	152days	01/06/2022	29/12/2022	35,36	
25	WP3 Demonstration and Testing (TUM)	804days	02/09/2019	29/09/2022		TUM
26	Demonstrator Baseline preparation (FLEXOP)	283days	01/06/2020	30/06/2021		TUM
27	Demonstrator prep FT #1	88days	01/06/2020	30/09/2020		TUM
28	Demonstrator prep FT #2	45days	29/04/2021	30/06/2021	36	TUM
29	Demonstrator Advanced Wing Design (Structure, Sensors, Data A	152days	02/07/2021	31/01/2022		TUM
30	Sensor Concept Design	41days	02/07/2021	27/08/2021	22	SZTAKI
31	Adv Wing Manufacturing Design	152days	02/07/2021	31/01/2022	22	TUM
32	Adv Wing Manufacturing and Integration	152days	30/08/2021	29/03/2022	30	TUM
33	Demonstrator Integration and testing (GVT, HILS, initial flight)	87days	30/03/2022	28/07/2022	31,32	DLR
34	Flight Test Specification and System Identification Experiment des	631days	02/09/2019	31/01/2022		ONERA
35	Flight Test Programme Definition - FTC 1	88days	02/09/2019	01/01/2020		ONERA
36	Flight Test Programme Definition - FTC 2	43days	01/03/2021	28/04/2021	8,35	DLR
37	Flight Test Programme Definition - FTC 3	66days	01/11/2021	31/01/2022	36	TUM
38	Flight Test Campaign	521days	01/10/2020	28/09/2022		TUM
39	Flight Test Campaign 1	45days	01/10/2020	02/12/2020	27,35	TUM
40	Flight Test Campaign 2	46days	01/07/2021	02/09/2021	7,28,36,39	TUM
41	Flight Test Campaign 3	86days	01/04/2022	29/07/2022	37	TUM
42	Data preparation for ORD	44days	01/08/2022	29/09/2022	41	SZTAKI
43	WP4 Scale-Up (DLR)	365days	01/07/2021	23/11/2022		DLR
44	Aircraft design objectives	132days	01/07/2021	31/12/2021	2,3	DLR
45	Implementation of reference A/C into toolchain (Reference A/C)	41days	03/01/2022	28/02/2022	3,21,22,44	TUM
46	Avionics Systems Architecture Design (Scale Up)	44days	01/03/2022	29/04/2022	18,21,22,45	DLR
47	Perform design study	88days	02/05/2022	31/08/2022	46	ONERA
48	System Benefit Assessment (Scale Up)	66days	01/09/2022	23/11/2022	20,21,22,23,39,40	DLR
49	WP5 Management (SZTAKI)	868days	02/09/2019	28/12/2022		SZTAKI Managem
50	Project Management	761days	02/09/2019	01/08/2022		SZTAKI Managem
51	Collaboration Tools	127days	07/05/2020	30/10/2020		SZTAKI Managem
52	Dissemination and Exploitation	780days	02/01/2020	28/12/2022		SZTAKI Managem

PNG Generated On: 24/09/2020, 12:31:35

The current critical path in the project is related to the design, manufacturing and flight test of the -3 demonstrator wing, where the benefits of the MDO process are demonstrated. Based on the current plan, the flight testing of -3 has to start on March 2022, what is preceded by 3 months ground testing (static test, ground vibration test and sensor calibration). Before testing, 6 months are required to manufacture the wing, what leads to the requirement that the design should be ready by 30/06/2021. The current effort among the consortium focuses on meeting this target deadline, so the MDO workflow would be able to produce the results, and some of the less critical deliverables and tasks are shifted towards later date in the GANTT chart above. The scale-up study what would nominally start 01/07/2021 already started with selecting the candidate configuration and finding suitable aircraft mathematical models from DLR's inventory.

RECOVERY PLAN

The whole consortium is very committed about recovering from the delay and already implemented procedures to improve work distribution and adapt to the new situation.

Flight test was originally planned for 3 weeks slots within each year due to logistics and human power constraints. This is now being changed to allow flight testing whenever it is possible during the year between February and November. In parallel, the simulation platforms at TUM, DLR and SZTAKI are now being harmonised to allow development, testing and deployment on the demonstrator without the physical presence of the other partners at the various locations.

The consortium also made a plan for the next 9 months about the schedule of deliverables, what we plan to update and iterate regularly, as the situation evolves.

TIMELINE

Deliverables, Ethics, DMP, Other Reports							
WP No	Del Rel. No	Del No	Title	Description	Lead Beneficiary	Est. Del. Date (annex I)	updated delivery date
WP1	D1.1	D1	Wing and demonstrator actuation and sensing conceptual design require	The deliverable will	TUM	2020. 2. 29.	2020. 10. 31.
WP1	D1.2	D2	Requirements capture for a/c MDO design	The requirements fo	TUM	2020. 2. 29.	2020. 11. 30.
WP1	D1.3	D3	Demonstrator ground and flight test requirements definition	To be able to demo	MTA SZTAKI	2020. 12. 31.	2021. 1. 31.
WP1	D1.4	D4	Information and interfaces definition for Collaborative Work Process	The interdisciplinary	MTA SZTAKI	2021. 6. 30.	2021. 8. 31.
WP1	D1.5	D5	Reference Model Definition	Based on the expe	DLR	2020. 6. 30.	2020. 11. 30.
WP1	D1.6	D6	Data Analytics for Model Validation	The data from flight	MTA SZTAKI	2021. 12. 31.	2021. 12. 31.
WP1	D1.7	D7	Standardization recommendations for data and model databases and too	Based on the lesso	DLR	2022. 12. 31.	2022. 12. 31.
WP2	D2.1	D8	Report on flight control system layout	Report describing th	ONERA	2020. 6. 30.	2020. 12. 15.
WP2	D2.2	D9	Report on tool adaptation for collaborative design	The report will cons	TUM	2020. 5. 31.	2020. 10. 31.
WP2	D2.3	D10	Analytical redundancy methods	In order to achieve	MTA SZTAKI	2020. 12. 31.	2021. 7. 31.
WP2	D2.4	D11	Validation of the integrated design toolchain for collaborative design	Validation of the int	DLR	2022. 12. 31.	2022. 12. 31.
WP2	D2.5	D12	Aero-servo-structural design of the new advanced FliPASED wing	This report address	TUM	2022. 1. 31.	2022. 1. 31.
WP2	D2.6	D13	Validation of data science based methods for modelling and control	This report address	MTA SZTAKI	2022. 12. 31.	2022. 12. 31.
WP3	D3.1	D14	Flight Test Programme – Flight Test Phase #1	A detailed flight tes	ONERA	2020. 2. 29.	2020. 10. 15.
WP3	D3.2	D15	Flight Test Report – Flight Test Phase #1	Based on the Flight	TUM	2020. 7. 31.	2021. 2. 28.
WP3	D3.3	D16	Flight Test Programme – Flight Test Phase #2	A detailed flight tes	DLR	2020. 11. 30.	2021. 4. 30.
WP3	D3.4	D17	Sensor concept advanced wing finalized	Based on the flight	MTA SZTAKI	2021. 2. 28.	2021. 8. 31.
WP3	D3.5	D18	Manufacturing design for advanced wing	Based on the detai	TUM	2021. 4. 30.	2021. 12. 31.
WP3	D3.6	D19	Flight Test Report – Flight Test Phase #2	Based on the Flight	TUM	2021. 5. 31.	2021. 9. 30.
WP3	D3.7	D20	Manufacturing advanced wing finalized	The results of the m	TUM	2021. 9. 30.	2022. 3. 31.
WP3	D3.8	D21	Flight Test Programme – Flight Test Phase #3	A detailed flight tes	TUM	2022. 1. 31.	2022. 3. 31.
WP3	D3.9	D22	Advanced wing integration and ground test completed	Before closure of th	DLR	2022. 1. 31.	2022. 3. 31.
WP3	D3.10	D23	Flight Readiness Review Demonstrator with Advanced Wing	The flight readiness	TUM	2022. 2. 28.	2022. 4. 30.
WP3	D3.11	D24	Flight Test Report – Flight Test Phase #3	Based on the Flight	TUM	2022. 7. 31.	2022. 9. 30.
WP3	D3.12	D25	Flight Test Data published in Open Research Data format	The flight test data	MTA SZTAKI	2022. 8. 31.	2022. 10. 31.
WP4	D4.1	D26	Scale-up design objectives	Captures and desc	DLR	2021. 12. 31.	2021. 12. 31.
WP4	D4.2	D27	Scale-up aircraft re-design and control system lay-out	Control system lay-o	ONERA	2022. 8. 31.	2022. 9. 30.
WP4	D4.3	D28	Report on quantified design benefits, as compared with reference	The report assesse	DLR	2022. 12. 31.	2022. 12. 31.
WP5	D5.1	D29	Project Handbook	This document cont	MTA SZTAKI	2020. 1. 31.	2020. 9. 15.
WP5	D5.2	D30	Project webpage and social media	The project website	MTA SZTAKI	2020. 2. 29.	2020. 9. 15.
WP5	D5.3	D31	Data management plan	The DMP will provid	MTA SZTAKI	2020. 2. 29.	2020. 9. 15.
WP5	D5.4	D32	12 month Progress Report	The project coordin	MTA SZTAKI	2020. 9. 30.	2020. 11. 30.
WP5	D5.5	D33	Exploitation and Dissemination Plan	Exploitation goals o	TUM	2021. 8. 31.	2021. 8. 31.
WP5	D5.6	D34	24 month Progress Report	The project coordin	MTA SZTAKI	2021. 9. 30.	2021. 9. 30.
WP5	D5.7	D35	Workshop / Final Exploitation and Dissemination Report	Organization of an	TUM	2022. 12. 31.	2022. 12. 31.
WP5	D5.8	D36	Final Report	The project coordin	MTA SZTAKI	2022. 12. 31.	2022. 12. 31.
WP6	D6.1	D37	EPQ - Requirement No. 1	-Further information	MTA SZTAKI	2020. 8. 31.	2020. 9. 30.

ACTIONS

Part of the recovery plan is to involve more resources on all sides.

- DLR already offered extra manpower for the development of the common simulation platform – allowing remote work.
- DLR committed extra resources to harmonize the current MDO process at DLR-SR with the MDAX tool developed within another H2020 projects, what shows significant promise in simplifying the setup of the custom MDO environment.
- TUM allocated extra resources on flight testing, by training a new pilot who will reduce bottlenecks in the flight test campaign.
- Results and experience from another TUM internal project, related to ground control station and engineering analysis capabilities were also shared with the FLiPASED project, hence the need of custom software development will be reduced.
- SZTAKI also recruited new personnel on software and implementation aspects on the MDO toolchain and aims to improve its independence from centralised DLR cloud server-based implementation of the MDO software setup. In this way parts of the overall MDO toolchain can be tested onsite at SZTAKI without the IT assistance of DLR.
- The standalone, independent software stack will be also shared with TUM, and ONERA so they could also develop and test their individual tools without the need for help of the DLR IT infrastructure. This further reduces risks related to delays caused by home office at DLR sites and allows independence of partners.

The consortium implemented measures and set goals according to the original project duration, but planning for long term involves significant uncertainty due to the unusual circumstances. The delay is 3-4 months at the moment, which is not as significant as one would assume based on the delay in the deliverables, since technical work have been performed, just the bureaucratic and administrative parts suffered setbacks due to lack of access to office related services.

6.2 Use of resources

6.2.1 Unforeseen subcontracting

Not applicable

6.2.2 Unforeseen use of in kind contribution from third party against payment or free of charges

Not applicable

7 Deliverables

Del No.	Deliverable name	Lead beneficiary	Delivery date from Annex I	Actual delivery date	If deliverable not submitted on time: Forecast delivery date if appropriate	Comments
D1.1	**Wing and demonstrator actuation and sensing conceptual design requirements**	**TUM**	**29 Feb 2020**		**2020.12.02. (submitted)**	
D1.2	**Requirements capture for a/c MDO design**	**TUM**	**29 Feb 2020**		**2021.02.20. (submitted)**	
D1.5	**Reference Model Definition**	**DLR**	**30 Jun 2020**		**2021.04.15.**	**still pending**
D2.1	**Report on flight control system layout**	**ONERA**	**30 Jun 2020**		**2021.02.20. (submitted)**	
D2.2	**Report on tool adaptation for collaborative design**	**TUM**	**31 May 2020**		**2021.02.20. (submitted)**	
D3.1	**Flight Test Programme – Flight Test Phase #1**	**ONERA**	**29 Feb 2020**		**2020.11.19. (submitted)**	
D3.2	**Flight Test Report – Flight Test Phase #1**	**TUM**	**31 Jul 2020**		**2021.02.28.**	**still pending**
D5.1	**Project Handbook**	**MTA SZTAKI**	**31 Jan 2020**	**2020.09.11**		
D5.2	**Project webpage and social media**	**MTA SZTAKI**	**29 Feb 2020**	**2020.09.15**		
D5.3	**Data management plan**	**MTA SZTAKI**	**29 Feb 2020**	**2020.09.11**		

D5.4	**12 month Progress Report**	**MTA SZTAKI**	**30 Sep 2020**		**2020.10.15**	
D6.1	**EPQ - Requirement No. 1**	**MTA SZTAKI**	**31 Aug 2020**		**2020.09.30**	

8 Milestones

M No.	Milestone name	Lead beneficiary	Delivery date from Annex I	Means of verification	Achieved (Y/N)	If deliverable not achieved Forecast achievment date	Comments
MS1	**Aircraft / wing conceptual avionics design frozen**	**TUM**	**29/02/2020**	The aircraft configuration, including actuation, sensing and avionics are described according to the flight test campaign objectives. The milestone is reached by delivering D1.1.	Yes		The avionics design was frozen while working on D1.1 and D1.2 – to be aligned with both the currently existing demonstrator (and the improvements required w.r.t the FLEXOP project) and its future needs to show the benefits of the MDO tools.
MS7	**Flight Test Phase #1 completed**	**TUM**	**31/07/2020**	The first flight test campaign with baseline wing configuration is performed and the data is processed for further validation. The milestone is reached when all data is available for the flight test report (D3.2).	**No**	**June 2021**	The team attempted flight testing the demonstrator, but low speed handling problems (instability) led to hitting a light post at the airfield. Due to this the whole wheel assembly, as well as takeoff and landing procedures have been revised and critical components replaced. Due to restrictions related to COVID very limited opportunities were present to flight test the airplane. We tried to mitigate the software related bottlenecks by installing a second HILS simulator (for pilot training) at TUM.

MS4	**Methods and tools for MDO fixed**	**TUM**	**31/08/2020**	The individual design tools for all aeroservoelastic disciplines have to be fixed and the specifications in addition to common data exchange interfaces have to be defined to start the MDO design taking advanced movable design into consideration. The milestone is reached when the MDO iteration structure and its sub components are fixed and defined.	**Yes**		The milestone was reached when delivering D1.2, the individual tools and building blocks are agreed and the clear path and responsibilities for integrating them is established.

9 Dissemination and Exploitation of Results

9.1 Scientific publications

Authors / Speaker	Partner	Title	Conference / Journal	Date	Place	DOI
Matthias Wüstenhagen ; Özge Süelözgen ; Lukas Ackermann; Julius Bartaševicius	DLR, TUM	Validation and Update of an Aeroservoelastic Model based on Flight Test Data	AeroConf 2021 (IEEE)			
Balint Patartics, Gyorgy Liptak, Tamas Luspay, Peter Seiler, Bela Takarics and Balint Vanek	SZTAKI	Application of Structured Robust Synthesis for Flexible Aircraft Flutter Suppression	IEEE Transaction on Control System Technology Journal:			
Réka Mocsányi, Béla Takarics and Balint Vanek	SZTAKI	Robust Control Design for the FLEXOP Demonstrator Aircraft via Tensor Product Models	Asian Journal on Control			
Bauer, P ; Anastasopoulos, L ; Sendner, F-M ; Hornung, M ; Vanek, B	SZTAKI, TUM,	Identification and Modeling of the Airbrake of an Experimental Unmanned Aircraft	JOURNAL OF INTELLIGENT & ROBOTIC SYSTEMS			